Forecasting coastal overtopping at engineered and naturally defended coastlines

Stokes, Kit; Poate, Tim; Masselink, Gerd; King, Erin; Saulter, Andrew; Ely, Nick

Published in:
Coastal Engineering

DOI:
10.1016/j.coastaleng.2020.103827

Publication date:
2021

Journal Pre-proof

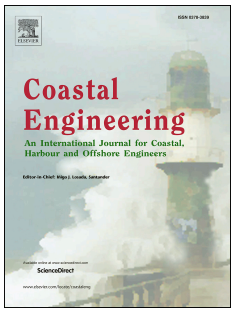

Forecasting coastal overtopping at engineered and naturally defended coastlines

K.I.T. STOKES, T.I.M. POATE, G.E.R.D. MASSELINK, E.R.I.N. KING, A.N.D.R.E.W. SAULTER, N.I.C.K. ELY

PII: S0378-3839(20)30513-5

DOI: https://doi.org/10.1016/j.coastaleng.2020.103827

Reference: CENG 103827

To appear in: *Coastal Engineering*

Received Date: 3 September 2020

Revised Date: 20 November 2020

Accepted Date: 29 November 2020

Please cite this article as: STOKES, K., POATE, T., MASSELINK, G., KING, E., SAULTER, A., ELY, N., Forecasting coastal overtopping at engineered and naturally defended coastlines, *Coastal Engineering*, https://doi.org/10.1016/j.coastaleng.2020.103827.

Author Contributions

- **Kit Stokes:** Conceptualization, Data curation; Formal analysis; Investigation; Methodology; Project administration; Software; Validation; Visualization; Writing - original draft; Writing - review & editing
- **Tim Poate:** Conceptualization, Data curation; Methodology; Project administration; Validation; Visualization; Writing - review & editing
- **Gerd Masselink:** Conceptualization, Data curation; Funding acquisition; Methodology; Project administration; Resources; Supervision; Writing - review & editing
- **Erin King:** Data curation; Formal analysis; Methodology; Validation; Writing - review & editing
- **Andrew Saulter:** Conceptualization, Data curation; Funding acquisition; Methodology; Writing - review & editing
- **Nick Ely:** Conceptualization, Funding acquisition

FORECASTING COASTAL OVERTOPPING AT ENGINEERED AND NATURALLY DEFENDED COASTLINES

KIT STOKES[1], TIM POATE[1], GERD MASSELINK[1], ERIN KING[1], ANDREW SAULTER[2], NICK ELY[3]

[1] School of Biological and Marine Sciences, University of Plymouth, Drake Circus, Plymouth, U.K.

[2] Met Office, Fitzroy Road, Exeter, Devon, EX1 3PB, U.K.

[3] Environment Agency, Sir John Moore House, Bodmin, Cornwall, PL31 1EB

Abstract

As sea level rises and development of the coastal zone continues, coastal flooding poses an increasing risk to coastal communities. Wave runup can contribute many meters to the vertical reach of the sea, especially on steep gravel beaches, and wave overtopping is a key contributor to coastal flooding along coastlines exposed to energetic wave conditions. However, operational forecasting of wave overtopping has rarely been attempted due to the need for high-resolution inshore water levels and wave conditions, up-to-date coastal profile and sea defence information, and availability of models or formulae that can robustly predict overtopping for a range of coastal profile types. Here, we have developed and tested an efficient forecasting system for providing operational warnings up to three days in advance for the entire 1000 km coastline of southwest England, called SWEEP-OWWL, which is capable of predicting wave runup elevation and overtopping volumes along the energetic and macrotidal coastline, featuring embayed, sandy, gravel, and engineered regions. Existing flood warning systems have used the process-based hydrodynamic model XBeach, but due to the computational cost, have resorted to populating look-up tables using off-line simulations and only a single realisation of the coastal bathymetry. Instead, SWEEP-OWWL runs in 'real-time' using a computationally efficient suite of empirical shoaling, breaking, runup, and overtopping equations at 184 coastal profiles, forced with hydrodynamic information from a regional 1-km spectral wave and hydrodynamic model. Importantly, the forecast system can be updated with the latest coastal profile data with no extra computational cost, which is shown to improve the accuracy of predicted overtopping rate by an order of magnitude in some cases. Compared to visual observations of flooding events from live streaming webcams around the southwest, the system correctly predicted the presence or absence of wave overtopping with 97% accuracy and showed skill in differentiating between low and high hazard events. Reliable forecasts of wave overtopping could considerably enhance a coastal community's ability to prepare and mitigate against the risk to life, property, and infrastructure during coastal flooding events, and the developed system shows that this can be achieved using a single desktop PC for entire regions featuring both natural and man-made sea defences.

1 Introduction

Coastal flooding occurs when water from the sea or ocean is able to overtop natural (e.g., beaches, sand dunes, gravel barriers, cliffs) or man-made (e.g. sea dykes, sea walls, rock revetments) coastal defences. This can occur due to a combination of tidal elevation, inverse barometric effect, onshore wind, and wave induced overtopping; over long time scales these processes are compounded by sea-level rise. There have been numerous significant coastal flooding events in the last century that have caused large-scale and extreme damage to property and infrastructure, disruption to coastal communities, and loss of life (for examples, seeVan Dongeren, Ciavola [1]). However, lower magnitude, but higher frequency, 'nuisance' coastal flooding events also cause disruption to coastal communities by closing transport links, flooding properties, and posing a safety hazard, and have become significantly more common in recent decades [2]. With rising sea levels, the frequency of both nuisance and extreme coastal flooding events is expected to increase in most places globally [2, 3]. For example, on the European Atlantic coast where this study was conducted, 10 cm of sea level rise is expected to occur by 2030 to 2050 and could double the frequency of extreme flooding events [3]. Where development of coastal areas continues unabated, the exposure to the hazard is increased, and the risk posed by coastal flooding will be exacerbated in the future.

Reducing coastal flooding risk requires a combination of measures to be taken, identified by [1] as prevention (engineering hard or soft sea defences), mitigation (preventing coastal development or relocating coastal communities), and preparedness (having forewarning of a flood event). The ability to forecast coastal overtopping several days in advance allows authorities to prepare for an event, for example by informing the type and location of emergency services that should be mobilised, or to prevent flood damage by informing where temporary flood defences should be deployed. This paper presents a new computationally efficient approach to forecasting coastal overtopping hazard for individual locations, across a large geographic region. The aim of the system is to enhance information available to coastal managers prior to a coastal flooding event and thereby increase the preparedness of coastal communities to such events.

Wave setup (the time-averaged super-elevation of the sea caused by wave breaking at the coast) and wave runup (the time-varying excursion of individual swash waves running up the coastal profile) can contribute many meters to the total elevation of the sea and are key contributors to coastal flooding along coastlines exposed to energetic wave conditions. For example, at coastal locations defended by gravel beaches or barriers, which are common in the UK, wave runup can be twice the magnitude of the significant wave height during a storm and has been observed to reach 12 m above still water level under extreme wave conditions [4]. This heightened elevation of water clearly increases the likelihood of overtopping and coastal flooding occurring (Figure 1). Large scale studies of future coastal flooding risk have mostly neglected the contribution of wave runup and overtopping due to the challenge of evaluating beach and sea defence geometries across large regions [2, 3, 5] and may therefore underestimate the likelihood of nuisance and even extreme coastal flooding. Operational ('real-time') forecasting of wave runup and overtopping over large regions (i.e. 100's of km) has only recently been attempted due to the need for high-resolution inshore water levels and wave conditions, up to date coastal topography and sea defence information, models or formulae that can robustly predict overtopping for a range of coastal profile types, and high performance computing.

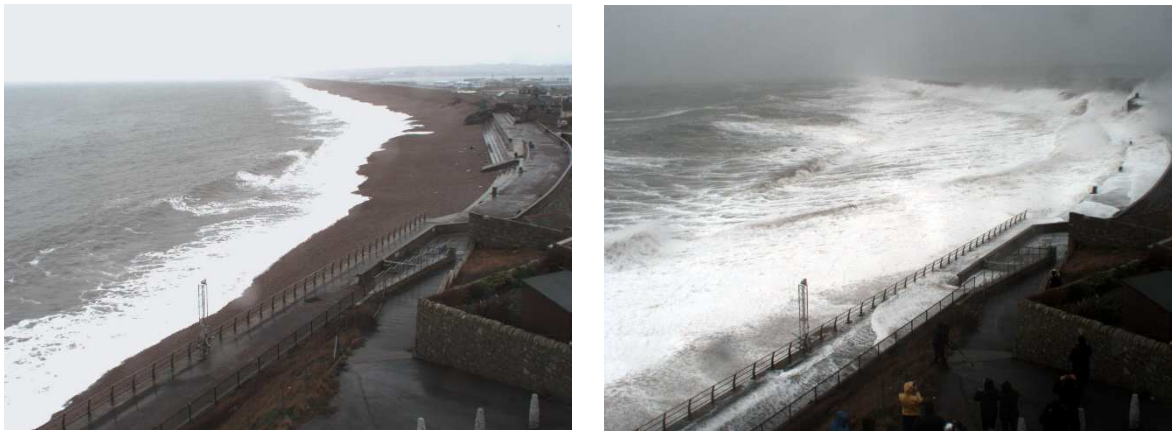

Figure 1. Wave runup at Chesil Beach, Dorset, UK, during storm Petra on the 5th of February 2014 (left) and overtopping occurring later during the same storm (right). Significant wave height was 8 m during the storm and wave runup height peaked at 12 m above the still water level, causing overtopping of the gravel barrier and flooding of the road, properties, and infrastructure behind the barrier.

Globally, there have been a number of previous efforts to forecast wave-induced coastal overtopping in real-time reported in the scientific literature [1, 6-9]. The early-warning systems developed in the USA (COSMOS project, [7]) and at multiple sites in Europe (RISC-KIT project, [1]; and UK by [9]) first downscale wave and meteorological conditions from global scale models to regional scale wave and hydrodynamic models (either Delft-3D [1, 7] or POLCOMS/ProWAM [9]), then to local 1D [9, 10] or 2D [11, 12] models where inshore wave conditions, wave overtopping, and morphological change are then modelled using process-based models such as XBeach [13] or RANS-VOF [9]. Process based models are too computationally expensive to run operationally for large 2D areas (e.g. km's) or for dozens of 1D profiles, and therefore both COSMOS and RISC-KIT used Bayesian Networks trained on the inputs (hydrodynamic boundary conditions and profile information) and outputs (coastal hazards) from a large number of offline XBeach simulations to predict flooding. The resulting systems therefore forecast coastal hazard with low online computational cost from a set of boundary conditions using a look-up-table approach.

Although this approach represents the physics of overtopping using process-based models that have proven highly effective at simulating either storm hydro- and morpho-dynamics at natural beaches [14-17] or wave overtopping of sea defences [9], there are limitations to using such models to forecast coastal flooding. Firstly, XBeach has not yet been developed to simulate overtopping for man-made sea defences – for example, a wave return lip cannot be represented and airborne spray is not resolved – and overtopping predictions have rarely been tested against observations. Secondly, it is computationally expensive to run process-based models including XBeach and RANS-VOF for large regions, e.g. 100's of km [18]. Thirdly, the results are dependent on the nearshore bathymetry/topography used in the model (Section 4.4) and the offline simulations are only therefore relevant close to the time at which the bathymetry was measured. Re-running the offline simulations with updated bathymetry would incur significant additional computation time with each update.

Another approach to forecasting coastal overtopping that overcomes some of these limitations is to apply parametric wave runup and overtopping formulae to measured coastal profiles [6, 8]. Empirical overtopping formulae determined from scaled physical models and field data are available for a wide variety of

environmental conditions and coastal profile types, including most common sea defence structures [19], and the application of such equations is the standard approach for the assessment of future coastal flood risk and for engineering new sea-defence schemes. Surprisingly, however, this approach has rarely been applied to operational forecasting of coastal flooding. An existing precedent for this approach is the comparison of predicted runup heights to dune crest elevations from Lidar data to generate a binary warning system for overwash occurrence [6] which has been applied along naturally defended parts of the U.S. coastline [20]. More recently, [8] developed and validated a forecast of wave runup height for sloping sea walls to provide forewarning of potential overtopping in Taiwan, and even forced their parametric runup equations with ensemble wave model outputs to provide excellent predictive skill. However, their approach did not attempt to directly predict overtopping volume or hazard, and was limited to sloping seawalls and therefore did not deal with the full spectrum of sea-defence types encountered along most coasts. Therefore, a parametric forecasting approach that uses an suite of equations to efficiently generate overtopping warnings for naturally defended and engineered profiles across an entire region, has not previously been achieved.

In this contribution, an operational, real-time coastal flood warning system for southwest England has been developed as part of the South West Partnership for Environment and Economic Prosperity (SWEEP; www.sweep.ac.uk) project, funded by the UK's Natural Environment Research Council. The system is called the SWEEP Operational Wave and Water Level model (herein SWEEP-OWWL). It combines a process-based model to downscale regional forcing conditions, and a suite of parametric equations for wave shoaling, breaking, runup, and overtopping at the coast to forecast the level of overtopping hazard. As discussed later, the SWEEP-OWWL system enables the forecasting of coastal overtopping with relatively low computational cost, it can be 'bolted on' to any high-resolution wave model, and it can be updated with new coastal profile information without incurring any extra computational cost. The UK's Environment Agency (EA) and Met Office (MO) have partnered with SWEEP, and have assisted in the development of the coastal flood warning system to maximize the community preparedness gained from the system.

2 Regional setting

Forecasting wave runup and overtopping in southwest England requires a multi-pronged approach as flood protection along the ~1000 km coastline is provided by both natural and engineered defences (Figure 2). In many places the coast is protected by a combination of defence types (for example a sand or gravel beach backed by a seawall) adding to the complexity of forecasting coastal flooding. The wave-dominated north coast is predominantly defended by sandy beaches backed by dunes or vertical seawalls, and becomes progressively more tidally-dominated towards the northeast part of the region, where mud flats backed by revetments become more common in the mouth of the Severn Estuary. The south-facing coastline is divided by three large peninsulas (Portland Bill, Start Point, and Lizard Point; shown at 1, 60, and 94 in Figure 2) with significant variation in wave exposure within each intervening embayment: the west-facing areas are exposed to Atlantic swell and are often defended by sandy or gravel beaches, while the east or south facing areas feature seawalls and other hard defences. Current coastal flood warnings for the region, provided by the Environment Agency, consider forecasted tide and storm surge levels, and use expert opinion to estimate the additional hazard from

waves, but do not objectively predict the level of wave set-up, runup, and overtopping, which are key contributors to coastal flooding in the region.

The region experiences a meso- to macrotidal range that varies between 2 m (Portland, Dorset) to 12 m (Avonmouth, Bristol) on spring tides, and an energetic wave climate that receives long period swell waves and locally generated wind waves from the Atlantic Ocean, as well as easterly wind waves generated in the English Channel on the south-facing coastline. Waves in the southwest can get very large during extreme storms: one storm swell in October 2013, named 'Hercules', featured deep-water significant wave heights and peak periods measured off southwest Cornwall of H_{m0} = 9.6 m and T_p = 22 s, respectively [21]. To compare the levels of wave exposure within the region, the 1-year return period breaking wave height, H_{b1yr}, was estimated for each location in the study area over 40 years (Jan 1980 – May 2019, inclusive) of hindcast nearshore wave conditions generated using an 8-km resolution WAVEWATCH III model run at the UK Met Office [22]. Wave heights with a 1-year return period were determined from the nearshore hindcast using a Generalised Pareto Distribution fitted to peak wave heights exceeding the time series mean plus one standard deviation (with peaks separated by at least 4 days), before shoaling this wave height to a theoretical breaking wave height (Section 3.4). Figure 2 demonstrates that H_{b1yr} varies from < 0.1 m to 7.5 m in the region, while the elevation of Mean-High-Water-Spring (MHWS) tides varies from 1.8 to 6.3 mODN. Sea defence crest freeboard R_c above MHWS for the natural and man-made defences in the region varies from close to zero in some places, to more than 15 m in others.

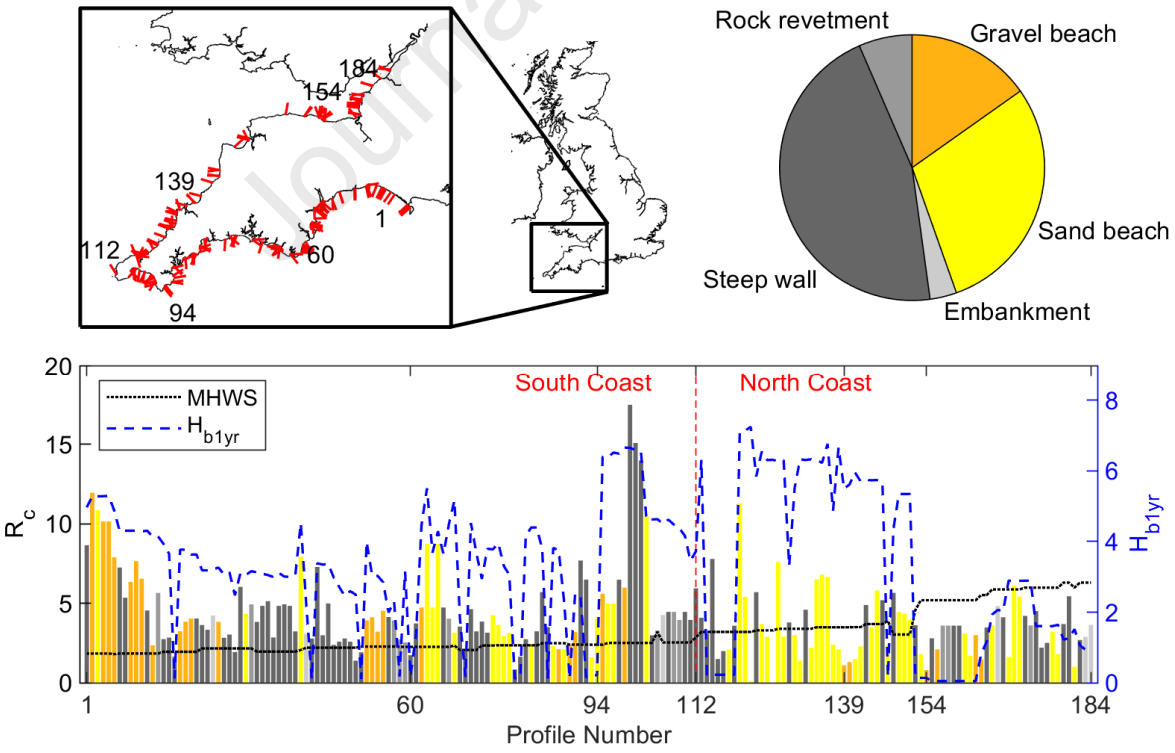

Figure 2. Top left panel: geographic location of the study area in the UK and the 184 studied profiles (red lines, example profile numbers shown for reference to the bottom panel). Top right panel: proportion of natural and

man-made sea defence types for the 184 studied profiles. Bottom panel, left axis: bar plot showing sea-defence freeboard from MHWS (R_c) and sea defence type (coloured as per top right panel), and MHWS elevation from ODN (dotted line). Bottom panel, right axis: 1 year return period breaking wave height, H_{b1yr} (dashed line).

3 Methodology

3.1 Overview of the modelling system

The SWEEP-OWWL coastal flood forecast is generated in three main stages (Figure 3). First, wave and water-level conditions around the coast of southwest England are forecasted using a 1-km resolution coupled wave and hydrodynamic model (Delft-3D), which downscales forcing data from a coarser 7-km north-west Atlantic shelf model run by the UK Met Office and propagates the forecasted waves and water levels in to the coast (Section 3.3). Second, the inshore wave conditions are empirically shoaled to the required depth (Section 3.4) and applied to an extensive database of measured coastal profile data (Section 3.2) using parametric equations to predict wave runup elevation and overtopping volume (Sections 3.5 and 3.6). Thirdly, the predictions are categorised into a level of coastal flooding hazard (Section 3.7) and are presented in synoptic regional and sub-region maps, as well as detailed time series plots for each coastal profile over the 3-day forecast window (Section 4.4). The wave and hydrodynamic model takes approximately 2.5 hours to complete a 4-day simulation, using 8 cores and parallel computing. The computation of wave runup and overtopping for 184 coastal profiles then takes less than 8 minutes using a single computational core.

3.2 Database of coastal profiles

A database of 184 topographic profiles representing the most at risk locations across 112 towns and beaches along the ~1000 km coastline was collated (Figure 2). These profiles are used to quantify intertidal slope, and the elevation of beaches, dunes and engineered structures for the prediction of wave runup and overtopping. Most profiles are measured down to Mean Low Water Spring (MLWS) elevation bi-annually by the Plymouth Coastal Observatory (PCO; https://www.channelcoast.org/southwest/) and are updated following extreme storms, and can therefore easily be updated in the SWEEP-OWWL forecast as new data are collected. As the PCO archive contains profile data every 50 m along the coast in most locations, only a selection of profiles were chosen from their archive. For each coastal location, one or more profiles were selected based on the type of sea defence present (natural or man-made), the amount of urbanization at risk, as well as the frequency of data collection at that profile. If multiple profiles existed in an urbanized location and shared a common sea defence type with the same crest elevation, then only the profile with the most frequently updated profile measurements was selected for inclusion in the database. Conversely, in locations where differing levels of coastal defence or wave exposure exist, multiple coastal profiles may have been included for a single town or village. In addition to the profile elevation data, information on the characteristics of the coastal structure was also collated from the PCO archive, LiDAR data, or freely available imagery.

3.3 Modelling nearshore waves and water levels

A coupled, 1-km resolution wave and hydrodynamic model was developed in Delft-3D [23] for the southwest of the UK (Figure 4). Delft-3D was chosen for this purpose as it computes both wave and tide driven hydrodynamics – both of which are significant in the southwest region (mean spring tide range 4 – 12 m, H_{b1yr} 0.2 – 7 m, Figure 2) – as well as their interaction, and, unlike some other similar models (e.g. MIKE) the software is available open-source, encouraging repeatability of the presented system in other locations. The core Delft-3D model was based largely on the model described in [24], with the addition of spectral wave forcing data and a 1-km resolution for both the wave and flow aspects. The primary purpose of this core model is to take offshore waves, water levels, and currents, and propagate them in to the coast using a relatively high-resolution grid, resolving the hydrodynamics at a sufficient resolution to differentiate the conditions occurring within each embayment around the southwest coastline. The Delft-3D model consists of two modules: a hydrodynamic model that computes water levels and currents using the non-linear shallow water equations ('D3D-flow'), and a third-generation spectral wave model ('D3D-wave') based on SWAN. These modules communicate with one another to allow for wave-current interactions to occur.

The core Delft-3D model obtains its boundary forcing conditions from larger area models run by the Met Office on behalf of the Copernicus Marine Environment Monitoring Service for the northwest European shelf (https://marine.copernicus.eu/about-us/about-producers/nws-mfc/). In the present set-up, Met Office global atmosphere and northwest European shelf hydrodynamic boundary conditions are provided on a 7-km resolution hydrodynamic model grid [NEMO 'AMM7'; 25], whilst spectral wave boundary conditions are provided from a 1.5-km model run by Met Office in the UK [WAVEWATCH III 'AMM15'; 22]. These larger models provide 2D spectral wave data, water levels, and currents to drive the four model boundaries, as well as gridded wind and pressure data across the entire domain to allow wind wave growth and barometric effects within the 1 km Delft-3D model. A routine was developed in Matlab which runs automatically every day and retrieves the latest Met Office forcing data from an FTP server, prepares all model input files, runs the Delft-3D model, and generates a fresh one-day hindcast and three-day forecast within the 1-km SWEEP-OWWL model domain. Validation of the Delft-3D model is presented in Section 4.1 of this paper. The 1-km wave and hydrodynamic model takes approximately 2.5 hours to complete a 4-day simulation (1-day hindcast plus 3-day forecast), using 8 cores and parallel computing.

Having shoaled the waves from the model boundary into shallow water at the coast, wave and water-level conditions are output along the 10, 15, and 20 m depth contours at approximately 1-km spacing, providing inshore conditions in each embayment along the coastline. Output is selected from the shallowest depth contour at which depth-induced wave breaking has not yet occurred, which is conservatively indicated by significant wave heights at the output location that are less than half the water depth, as this is well below typical values used for breaker criterion [for example, 26]. For example, for wave conditions of up to 5 m H_{m0}, output is taken from the 10 m depth contour, and for more extreme wave conditions the 15 or 20 m contours are used. This approach enables the wave conditions to be extracted from the model as close to the coast as possible – allowing shoaling, refraction, and wave shadowing within embayments to occur – but prior to wave breaking, a process which the 1-km model grid would not sufficiently resolve.

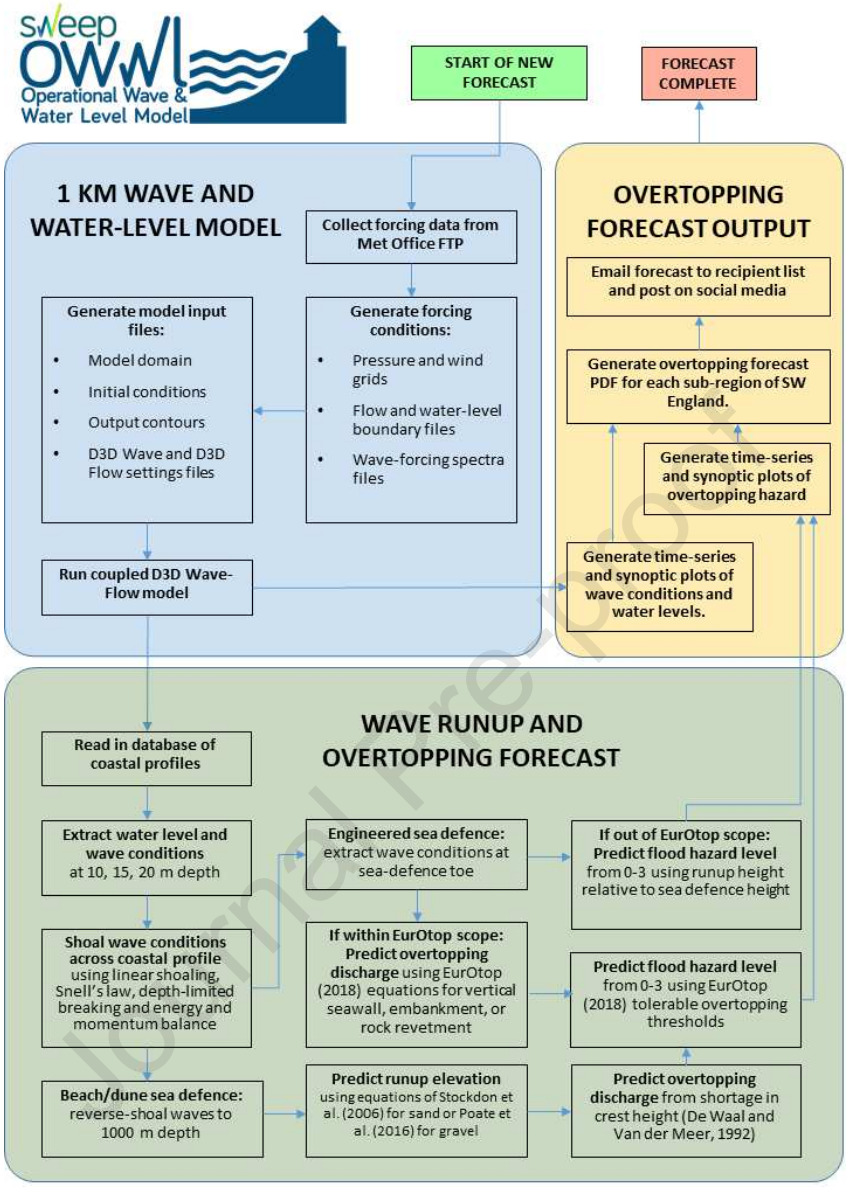

Figure 3. Flow diagram describing the main stages of SWEEP-OWWL: generating a wave and water-level simulation, predicting wave runup and overtopping, and outputting a coastal flood forecast.

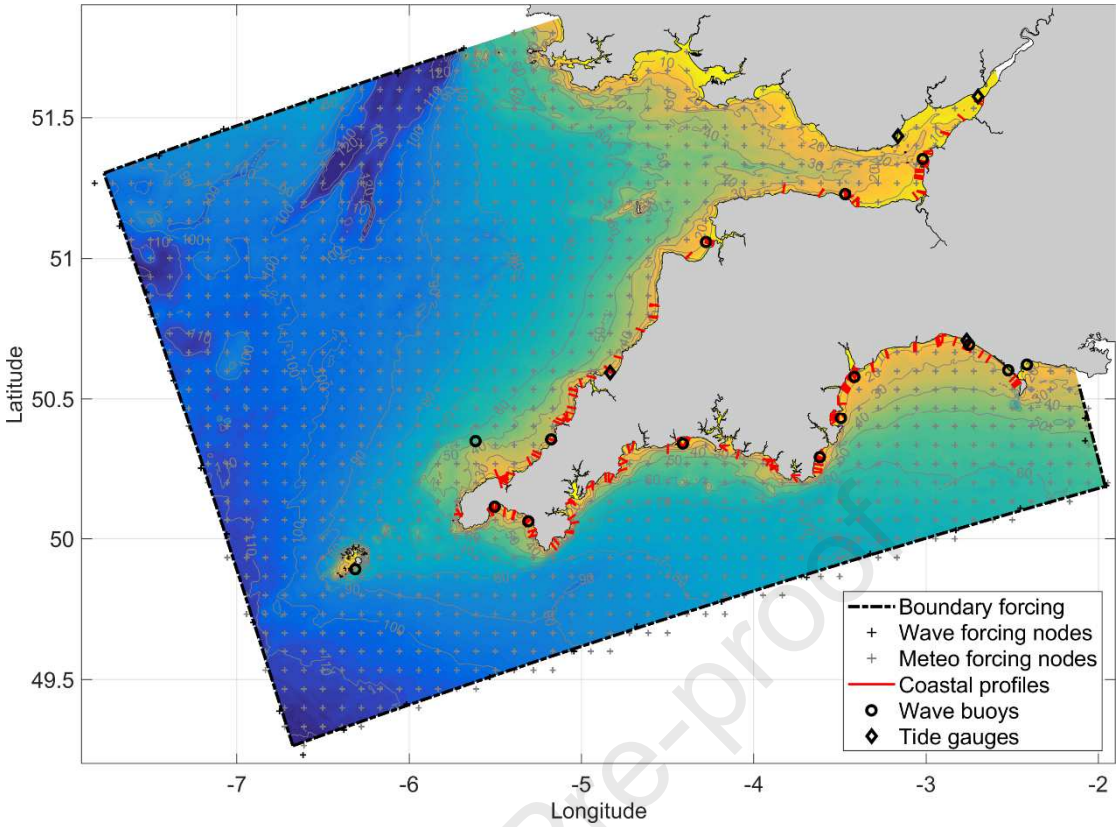

Figure 4. SWEEP-OWWL Delft-3D model domain, with bathymetric depth shown by shaded and labelled depth contours (mODN). Forced boundaries are indicated along the sides of the model domain. The location of wave buoys and tide gauges used for model validation are shown, as well as coastal profiles used to predict runup and overtopping (provided freely by the Channel Coastal Observatory; http://www.channelcoast.org/).

3.4 Modelling wave shoaling, breaking and set-up

To predict wave overtopping at sea-defence structures (Section 3.6.1), accurate estimates of the water level and wave conditions at the toe of the structure are required. To achieve this, parametric formulae were used to describe wave shoaling and breaking as well as wave induced set-up across each of the measured coastal profiles (Section 3.2) around the southwest coastline.

As wave conditions were output from the Delft-3D model beyond the seaward extent of the measured coastal profiles (which cover the intertidal beach down to MLWS), the profiles were artificially extended to the output depth using the distance to the output node and (time-varying) output depth to define the nearshore gradient. Wave breaking and decay was then modelled across each of the extended coastal profiles using the parametric breaker dissipation model described by Janssen and Battjes [27], which is an update to earlier breaker models [28, 29] and is notably more stable on steep beaches (herein referred to as JB07). The cross-shore (x) evolution of the wave energy flux, $Ec_g cos\theta$, was estimated from the mean rate of energy dissipation in a breaking wave, ε_b, and energy loss due to bed friction ε_f as:

$$\frac{\partial Ec_g cos\theta}{\partial x} = -\langle \varepsilon_b \rangle - \langle \varepsilon_f \rangle \quad (1)$$

where θ is the mean wave angle from shore normal; c_g is the wave group celerity described from linear theory as $c_g = c\left[\frac{1}{2} + \frac{kh}{sinh(2kh)}\right]$, with c, k, and h, the local wave phase speed, wave number, and water depth, respectively; and wave energy is found from linear theory as $E = \frac{1}{8}\rho g H_{rms}^2$, where ρ is water density, g is acceleration due to gravity, and H_{rms} is the root-mean-square wave height.

Wave energy dissipation was then modelled across the profile assuming a Rayleigh wave height distribution [27]:

$$\langle \varepsilon_b \rangle = \frac{3\sqrt{\pi}}{16} B \bar{f} \rho g \frac{H_{rms}}{h}\left[1 + \frac{4}{3\sqrt{\pi}}\left(R^3 + \frac{3}{2}R\right) exp[-R^2] - \mathrm{erf}(R)\right] \quad (2)$$

where B is a tunable coefficient approximately equal to 1 that controls the intensity of wave dissipation, $\bar{f}$ is a representative wave frequency here defined as the inverse of the peak wave period T_p, $R = H_b/H_{rms}$ where H_b is the depth-limited upper wave height at a given location, and erf represents the error function. Following [29] and [27], H_b and breaker criterion γ were defined using deepwater (denoted by subscript 0) wave steepness, $S_0 = H_{rms,0}/L_{P,0}$, estimated by reverse shoaling the nearshore wave conditions to deepwater wave height ($H_{rms,0}$) and wavelength at the peak of the spectrum ($L_{P,0}$), and computing γ as:

$$\gamma = \frac{H_b}{h} = 0.39 + 0.56\tanh(33S_0) \quad (3)$$

Water depth h includes the still water depth d and wave-induced set-up $\bar{\eta}$ as $h = d + \bar{\eta}$. $\bar{\eta}$ was assumed to be zero at the Delft-3D model output location (beyond the surf-zone) and was then solved for across each extended coastal profile using a one-dimensional momentum balance following [30]:

$$\frac{\partial S_{xx}}{\partial x} + \rho g(h + \bar{\eta})\frac{\partial \bar{\eta}}{\partial x} = 0 \quad (4)$$

where the cross-shore component of radiation stress is given by:

$$S_{xx} = \left(\frac{1}{2} + \frac{2kh}{\sinh 2kh}\right) E \quad (5)$$

The water level corrections were then incorporated iteratively into Eq. 2 until the value of $\bar{\eta}$ converged at each cross-shore location, changing less than 0.01 mm between iterations.

Frictional losses were calculated across each extended coastal profile as [e.g. 13]:

$$\varepsilon_f = \frac{2}{3\pi}\rho f_w \left(\frac{\pi H_{rms}}{T_{m01}\sinh kh}\right)^3 \quad (6)$$

Where T_{m01} is the mean wave period and the wave-related friction coefficient f_w was estimated following [31]. Due to the artificial seabed profile used between the Delft-3D model output nodes and the seaward extent of the measured coastal profiles, it is acknowledged that our approach currently neglects wave dissipation over subtidal sandbars, which are typically shallower than the Delft3D output depth (and would not be resolved by

the 1 km model resolution) yet typically deeper than the MLWS extent of the measured profiles. This limitation could be remedied in future if more complete coastal profiles become available, and is expected to presently result in a conservative (over-) estimate of wave height at locations featuring nearshore bars, such as the intermediate beach types common on the north coast of Cornwall.

3.5 Predicting runup elevation

Almost all coastal profiles in southwest England include some form of intertidal beach slope; therefore, it is useful to predict the wave runup elevation as an initial indicator of coastal flooding hazard, especially for locations without an engineered sea-defence. The 2% runup exceedance height $R_{2\%}$ is a common means of quantifying the largest wave excursions and includes the contribution from both wave setup and runup, making it a useful indicator of the elevation at risk from overtopping (Figure 5). These processes are primarily governed by the relative magnitudes of the beach slope and the offshore wave steepness, and information about each is therefore required to make a prediction of runup at the coast. In SWEEP-OWWL, the formula of Stockdon *et al.* [32], determined through 10 dynamically different field experiments conducted at full scale on 6 sandy beaches in Holland and the USA, is used to predict wave runup elevation at sandy beaches:

$$R_{2\%} = 1.1\left(0.35\tan\beta\,(H_0L_0)^{1/2} + \frac{[H_0L_0(0.563\tan\beta^2+0.004)]^{1/2}}{2}\right) \quad \text{for } \xi_0 \geq 0.3 \tag{7}$$

and

$$R_{2\%} = 0.043(H_0L_0)^{1/2} \quad \text{for } \xi_0 < 0.3 \tag{8}$$

where H_0 is the deep-water significant wave height, L_0 is the deep-water wave length, and ξ_0 is the deep-water Iribarren or surf-similarity parameter [33], computed as:

$$\xi_0 = \frac{\tan\beta}{(H_0/L_0)^{1/2}} \tag{9}$$

For sediments ranging from fine gravel to large pebbles, the formula of Poate *et al.* [4] was used, which was determined from 10 different full-scale field experiments at 6 field sites in the UK along with nearly 15,000 XBeach-G [34] simulations:

$$R_{2\%} = 0.33\tan\beta^{1/2}\,T_pH_0 \tag{10}$$

For both the Stockdon and Poate runup equations, deep-water wave conditions were determined from the previously estimated breaking wave conditions at the coast (Section 3.4) by reverse-shoaling to a depth of 1000 m using linear wave theory. This ensures that the wave conditions used in the runup equations have undergone all major refraction and shoaling effects before the equivalent deep-water conditions are calculated. Using the reverse-shoaled deep-water wave conditions and the local beach gradient around the still water level (as prescribed in [32] and [4]), the wave runup elevation at the coast is predicted over the forecast window and added to the still water level to enable a forecast of the Total Water Level, TWL, through time.

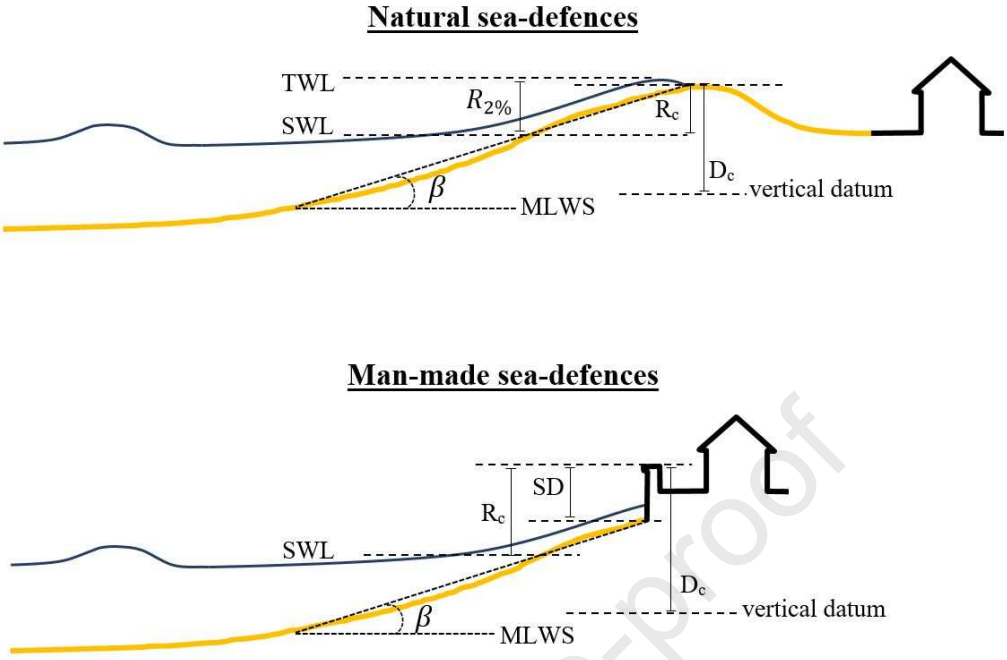

Figure 5. Definition of water level and sea defence geometric parameters for natural sea defences (beaches, dunes, and gravel barriers), and man-made sea defences (sea walls, rock revetments, and embankments). TWL = total water level (including wave setup and runup); SWL = still water level (including wave setup); $R_{2\%}$ = wave runup height; R_c = crest freeboard; D_c = crest elevation; β = beach slope between Mean Low Water Spring (MLWS) elevation and beach crest; SD = sea-defence height.

3.6 Predicting overtopping discharge

3.6.1 Man-made sea defences

For coastal profiles that feature a sea-defence structure, the volume of water overtopping the sea defence was predicted using various formulae from the EurOtop manual [19]. The equations in EurOtop have been determined through scaled and prototype-scale physical modelling of sea defences under wave attack, and EurOtop's 'mean value approach' is used in SWEEP-OWWL to predict overtopping discharge based on the best fit to each experimental dataset. The various equations for embankments, rock revetments, and vertical seawalls were coded into the SWEEP-OWWL model, using a decision-tree process to determine which equation is to be used for a given profile at a given point in time. The equations in EurOtop vary depending on the structure type, beach form, and forcing conditions, and, for brevity, the equations used in SWEEP-OWWL cannot all be reproduced here; however, the general approach is that the time-averaged overtopping discharge Q (m^3s^{-1} per m crest width) decreases exponentially as crest freeboard R_c increases, given as:

$$\frac{Q}{\sqrt{gH_{m0}^3}} = a\exp[-(b\frac{R_c}{H_{m0}})^c] \text{for } R_c \geq 0 \quad (11)$$

where H_{m0} = spectral significant wave height, and a, b, and c are fitted coefficients which vary depending on the structure type and forcing conditions. The left hand side of Eq. 11 represents the wave overtopping discharge normalised by wave height, while the right hand side represents the crest freeboard normalised by wave height.

Depending on the sea-defence geometry and forcing conditions, the right hand side of Eq. 11 is adjusted using coefficients termed 'influence factors', such as γ_b, γ_f, γ_v, γ_β, γ_{bn}, and γ_w that correct the wave overtopping discharge for the influence of a berm, slope roughness, a crest-top wall, oblique wave attack, a wave return lip, and strong onshore winds, respectively. Where possible, influence factors were quantified for each situation, but not all factors parameterized in the EurOtop manual could be determined from a desktop assessment of each coastal profile. In SWEEP-OWWL, berm width was ignored for all structures ($\gamma_b = 1$), as was surface roughness on embankments (γ_f = 1), but was conservatively set to $\gamma_f = 0.6$ for roughness on rubble mound structures [19 - table 6.2] and adjusted for wave steepness using Eqs. 6.1 and 6.7 from EurOtop [19]. In the case of a storm wall atop an embankment (γ_v), overtopping was decreased exponentially with the height of the storm wall relative to the crest freeboard, according to Eq. 5.45 of EurOtop [19]. Oblique wave attack (γ_β), informed by modelled wave conditions at the structure toe (Section 3.4), was adjusted for using EurOtop Eqs. 5.29 for embankments and seawalls and 6.9 for rock revetments. The influence of a wave return lip (reducing overtopping) or landward sloping parapet (increasing overtopping) was included in a simplified manner as $\gamma_{bn} = 1.1$ for a parapet and $\gamma_{bn} = 0.7$ for seawalls with a relative freeboard > 1 that feature a wave return lip, as per EurOtop Eqs. 7.21 and 7.22. More detailed adjustments for γ_{bn} are available that could be applied to SWEEP-OWWL when more detailed sea-defence geometries are available throughout the region.

In tests of the SWEEP-OWWL system, overtopping enhancement due to onshore winds combined with impulsive breaking using $\gamma_w = 2$ was found to produce unrealistically high overtopping volumes in many cases and the effect of wind on overtopping was therefore disregarded ($\gamma_w = 1$). The influence of a shallow foreshore, a toe mound in front of a seawall, or 'impulsive' wave breaking (when breaking occurs directly onto the sea defence) were included in SWEEP-OWWL as per the guidance in EurOtop [19]. More complex structure geometries including promenades, storm walls with a bull-nose, stilling basins, perforated seawalls, steeply battered walls, and composite breakwater slopes could not readily be quantified for the entire southwest region, and such secondary structure geometries were therefore ignored, simplifying each structure to the more conservative equations for the basic geometry.

To account for rare situations where a sea defence is completely submerged by the still water level (i.e. has a negative freeboard, $R_c < 0$), an equation for weir-flow conditions was used to adjust the overtopping discharge [19]:

$$Q = 0.54\sqrt{g|-R_c^3|} \qquad \text{for } R_c < 0 \tag{12}$$

where $|-R_c|$ represents the absolute value of the (negative) freeboard. In such situations, the weir-flow discharge from Eq. 12 is added to the predicted wave overtopping rate (Eq. 11) with $R_c = 0$, as recommended by EurOtop [19], to capture both weir-flow and wave-induced overtopping.

The case of a sea-defence structure with an emergent toe (i.e. the entire sea defence is above still water level) is one that is scarcely dealt with in the literature, but can result in considerable wave overtopping when wave runup is significant and freeboard is low. For embankments, an emergent toe was dealt with by including the beach slope in the calculation of the sea-defence slope (the 'equivalent slope'), as per the method of [35] recommended by EurOtop [19]. In the case of a seawall with an emergent toe, [36] tested overtopping using a scaled model beach with a slope of 1:10 topped by an emergent seawall and showed that overtopping was comparable to that of a plain slope with the same freeboard. However, the tested slope was impermeable and precludes all but the steepest gravel beaches. Therefore, it is unknown how well their adjusted formula applies to sandy beaches with an emergent seawall, as the gradient would be much shallower, or to steep gravel beaches with an emergent seawall, where infiltration would strongly influence the degree of overtopping. There therefore exists no reliable method in the literature to predict wave overtopping at seawalls or rock revetments with an emergent toe. Instead, the TWL (still water level plus predicted runup elevation) was compared to the height of the sea defence, SD (Figure 5), and estimated thresholds based on the relative elevations were applied to generate a coastal flooding hazard level, as described in Section 3.7.

3.6.2 Natural sea defences

For profiles where protection from coastal flooding is provided by either a sandy beach, dune, or gravel barrier, formulae to predict wave overtopping are not provided in the EurOtop manual. Very few studies have contributed parametric equations for wave overtopping discharge along naturally defended coasts [20] and those available have verified their models against only a limited range of slopes and sediment sizes in scaled model tests [37, 38] or against proxies of overwashing from field observations [39]. Recent efforts have concentrated on the development of process-based hydrodynamic models for the description of overwash during storms [14, 34, 40, 41], but are less applicable to SWEEP-OWWL due to the associated computational cost. As a result, a satisfactory empirical formula for wave overtopping at naturally defended coastal profiles does not yet exist in the scientific literature.

For SWEEP-OWWL, the approach proposed by De Waal and Van der Meer [42] for coastal structures and irregular waves was used to predict overtopping discharge over naturally defended profiles. This method is attractive as it assumes that overtopping discharge is related to a 'shortage in crest height', R_*, which can be parameterised using the runup elevation predicted by a chosen formula (in this case Eqs. 7 and 8 for sandy beaches and dunes, and Eq. 10 for gravel beaches and barriers) relative to the crest height of the coastal profile, D_c, as [42]:

$$R_* = (R_{2\%} - D_c)/H_s \tag{13}$$

Therefore, it allows us to apply the best available estimate of the wave runup elevation, accounting for different sediment types (sand vs gravel), to the prediction of overtopping volume. Normalised overtopping discharge is then predicted with [42]:

$$Q_* = \frac{Q}{\sqrt{gH_s^3}} = 8e^{-5}\exp(3.1R_*) \tag{14}$$

In Eqs. 13 and 14, H_s was taken at the point of incipient breaking, mimicking the approach used in EurOtop for embankments where the foreshore slope acts as part of the sea defence. Eq. 14 was tested against data from scaled mobile-bed sand dune overtopping tests by [37] and was found to reproduce the trend of overtopping volume within an order-of-magnitude, but systematically underestimated the values in their tests. However, we adopt Eq. 14 rather than the adjusted form proposed by [37] as it was fitted to a larger dataset and agrees better with the overtopping hazard observed during storms Emma and Eleanor, described in Section 4.3. There are shortfalls with this approach; primarily that it hasn't been previously tested with Eqs. 7, 8, and 10, or tested at all against field data from gravel beaches. Additionally, it assumes the overtopping hazard occurs at the very crest of the beach, dune, or barrier profile, when in reality the urbanisation at risk is often some way behind the crest, and infiltration may lessen the chances of coastal flooding. Nonetheless, it provides a conservative and versatile means with which to achieve an estimate of overtopping discharge at naturally defended profiles and provided reasonable agreement with observed overtopping hazard at sandy and gravel sites during the two storms presented in Section 4.3.

3.7 Predicting overtopping hazard

For cases where it is possible to predict the overtopping discharge rate (Section 3.6), i.e. naturally defended beaches or sea defences within the scope of EurOtop (excluding sea walls that are emergent above still water level), the thresholds for tolerable overtopping discharge provided in Chapter 3 of EurOtop [19] were applied to categorise the predicted overtopping into a hazard level. These represent discharge rates at which overtopping becomes hazardous to certain elements at risk, including pedestrians, properties, and vehicles, and in some cases were derived from prototype-scale experiments [19]. The EurOtop thresholds were combined into a scheme of discharge rates (Table 3-1) that differentiate four different hazard levels, from 0 – 3, and recognises that larger waves can deliver a larger instantaneous overtopping volume and therefore pose a greater hazard. The predicted discharge volume Q (Section 3.6) is first multiplied by 1000 to provide units of $ls^{-1}m^{-1}$, and is then assigned a hazard level using the thresholds summarised in Table 3-1. [19] suggests that little hazard is posed when $H_{m0} < 1$ m and 'low hazard' (level 0) is therefore assigned in such situations, except when freeboard is negative and weir flow conditions are predicted ($R_c \leq 0$; Eq. 12). To ensure the discharge thresholds are monotonically increasing, it was necessary for the thresholds for hazard level 1 with $H_{m0} < 3$ m to be more conservative than those recommended by EurOtop, and the level 1 threshold for $H_{m0} > 3$ m was applied in such cases (Table 3-1).

Beaches where a sea wall is present but completely emergent above the still water level (depicted in Figure 5, lower panel) represent the most poorly understood cases for predicting wave overtopping. Comparison of MHWS water level to seawall toe elevation indicates that 51 of the 81 studied seawalls in SW England (Figure 2) are emergent throughout the tide, with toe elevations 0.2 – 6.3 m higher than MHWS prior to Storm Eleanor in January 2018 (see Section 4.3). In fact, all of the studied seawalls become emergent at some point in the tidal cycle. In order to provide a continuous forecast of overtopping hazard, it is therefore vitally important to be able to predict overtopping for emergent seawalls. However, only a single such overtopping case has ever been tested [36] and as a result EurOtop does not yet provide a robust means of predicting overtopping discharge when still water level is below the toe of a seawall. To overcome this issue, a different approach to forecasting overtopping hazard was developed for this scenario. Hazard thresholds were estimated based on the predicted TWL, which

includes the still water level and theoretical runup height computed assuming no structure is present, relative to the toe-to-crest height of the sea-defence structure (SD, Figure 5). Hazard levels 1 and 2 are assigned to wave runup that exceeds the toe elevation plus ¼ and ½ of SD, respectively (assuming that spray overtopping occurs), while hazard level 3 is assigned to wave runup that exceeds the toe elevation plus SD (i.e. exceeds the crest elevation).

Table 3-1. Thresholds of overtopping discharge (Q, $ls^{-1}m^{-1}$) used to categorise hazard level, based on the tolerable overtopping rates recommended in EurOtop [19]. Low hazard level (level 0) is given when $H_{m0} < 1$ (m) and $R_c > 0$ or when the thresholds below are not exceeded.

Wave height and freeboard	Hazard to pedestrians (level 1)	Hazard to pedestrians & property (level 2)	Hazard to pedestrians, property & vehicles (level 3)
$1 \leq H_{m0} < 2$ & $R_c > 0$	0.3 (10 – 20 recommended)	1	75
$2 \leq H_{m0} < 3$ & $R_c > 0$	0.3 (1 recommended)	1	10 – 20
$H_{m0} \geq 3$ or $R_c \leq 0$	0.3	1	5

Table 3-2. Thresholds of total water level (TWL) used to categorise overtopping hazard where discharge rates cannot be predicted. SD is the crest elevation of the sea-defence structure. Low hazard level (level 0) is given when $H_{m0} < 1$ and $R_c > 0$.

Wave height	Hazard to pedestrians (level 1)	Hazard to pedestrians & property (level 2)	Hazard to pedestrians, property & vehicles (level 3)
All H_{m0}	¼ SD ≤ TWL < ½ SD	½ SD ≤ TWL < SD	TWL ≥ SD

4 Results

4.1 Delft-3D model validation

The Delft-3D model was validated using observed water levels, depth-averaged velocities and wave parameters using an extensive network of tide gauges, wave buoys and two ADCP deployments. Performance was determined using R-squared (R^2), bias, mean absolute error (MAE), Willmott Index of Agreement (WIA) and Brier Skill Score (BSS), calculated using the methods described in [24]. BSS was determined using a linear fit as a reference model [43] and computed following [44]. The hydrodynamic model component mirrors the hydrodynamic component of the regional model presented by [24], where a full validation between September 2013 and June 2014 is presented. Water levels were validated at eight tide gauges and were reproduced with excellent skill at all locations with the exception of Weymouth, where a double-low water component of the tidal oscillation is missed due to proximity and location of the eastern domain boundary at that site. The high water signal is reproduced well at all sites and the aggregated Brier skill score (BSS) was 0.99 with a bias of -13 cm. The residual elevations determined from low-pass filtering and from harmonic analysis tend towards slight underestimation, with an aggregated bias of −13 cm (low-pass filtering) and −3 cm (harmonic analysis). Depth-averaged current velocities are simulated with good skill overall (east component: BSS = 0.76, bias = 3 cm s^{-1}; north component: BSS = 0.68, bias = 2 cm s^{-1}).

The wave model in SWEEP-OWWL differs slightly from [24], featuring a higher spatial resolution and use of spectral wave forcing and wind forcing. As such, the wave component was further validated over two energetic epochs in 2018 from 03/01 to 09/01 (including storm Eleanor - Section 4.3) and from 17/02 to 07/03 (including storm Emma - Section 4.3). Observations of H_{m0}, peak and mean wave period (T_p and T_m, respectively) and mean wave direction (D_m) from thirteen wave buoys were used for comparison with the model, which was run using one-day-ahead forcing conditions. The validation was influenced by both the accuracy of the predicted forcing conditions and the accuracy of the wave propagation and shoaling in the Delft-3D model, and represents the expected skill of the forecasted nearshore conditions one-day-ahead. Validation statistics for the aggregated wave buoy data from all buoys in Figure 4 are presented in Table 4-1 for both epochs. Considerable scatter in T_p, T_m and D_m was observed in the buoy data for H_{m0} < 1m and these data were excluded from the validation. The wave model predicted H_{m0} excellently (BSS > 0.8) for both epochs, with a slight positive bias. T_p was predicted with reasonable to good skill for both epochs (0.4 < BSS < 0.8). Mean period T_m was better predicted with BSS indicating good skill across both epochs (BSS > 0.6). MAE was lower for T_m than T_p, with the greatest MAE for T_p during Epoch 1 at 2 seconds. D_m was predicted with excellent skill by the model (BSS > 0.9, MAE < 15°), with an improvement in skill for the higher energy epoch (03/01 to 09/01). Model error relative to the observations was less than half of the observed deviations about the observed mean for all variables, as indicated by the WIA > 0.5. Good to excellent predictive skill for H_{m0}, $D_{m,}$ and T_m, and reasonable to good skill for $T_{p,}$ indicate the suitability of this wave model as a predictive tool.

Table 4-1. Validation results of Delft-3D wave model output compared to inshore wave buoy measurements (locations given in Figure 4). * indicates circular correlation coefficient used for directional data.

	Epoch 1 (Storm Eleanor)						Epoch 2 (Storm Emma)					
Variable	N	R^2	BIAS	MAE	WIA	BSS	N	R^2	BIAS	MAE	WIA	BSS
H_{m0} (m)	4081	0.89	0.32	0.41	0.79	0.86	10877	0.82	0.16	0.27	0.76	0.85
T_p (s)	2454	0.52	0.42	2.06	0.67	0.57	4595	0.71	-0.39	1.21	0.78	0.74
T_m (s)	2454	0.75	0.49	0.85	0.66	0.78	4595	0.64	0.09	0.69	0.67	0.62
D_m (°)	2454	0.88*	-0.48	14.04	0.88	0.92	4595	0.76*	-2.42	14.98	0.89	0.90

4.2 Wave overtopping validation – daily observations

Collecting quantitative overtopping observations at field-scale is notoriously challenging, as well as expensive. This has previously been achieved at a small number of individual locations; for example, either a large container has been used to catch and measure overtopped water [19], or an array of capacitance wires at the sea-wall crest [45, 46], or in-situ laser scanner near the crest of a natural barrier [47] have been used. These approaches were not deemed feasible for the validation of the present overtopping forecast, given the geographic extent of the study, although ongoing research will use capacitance wire technology at two locations in the region for this purpose. Instead, to determine the ability of the present forecast to provide forewarning of overtopping for coastal management purposes, the predictions were here subjectively assessed using live-streaming webcams at 15 locations around the coast (Figure 6). Each webcam showed the first line of coastal defence (natural or man-made) in the field of view, and each day over a five month period (09/11/2018 – 06/04/2019), the predicted hazard level was compared to a subjectively ranked hazard observation made using each webcam. Due to a lack of suitable webcams at sites featuring embankments or rock revetments, only sites with seawalls (n = 9), sandy beaches (n = 3), and gravel beaches (n = 1) were included in the overtopping validation. Each webcam was accessed once a day at the time of a high tide, or at the time of predicted peak flooding, which was sometimes up to an hour either side of high tide, and was viewed for around 10 minutes to assess the level of overtopping. The observed overtopping was then subjectively ranked on a scale of 0–3, as per the flood hazard descriptions in Table 3-1, before noting the one-day-ahead forecasted hazard level. Apart from timing the observations to coincide with predicted overtopping peaks, the ranking was conducted without prior knowledge of the forecasted hazard level. It is acknowledged that the observations are highly subjective and that it is difficult to visually assess overtopping hazard. However, given the difficulty and expense involved with collecting quantitative overtopping observations at multiple locations, this approach was deemed the only feasible way to validate the system on a regional scale. It should be noted that while the subjective ranking of overtopping provides a useful comparison to the overtopping forecast, the actual overtopping volumes are not known and therefore it is possible that the forecast could be more accurate than the observations, or vice versa, on any given day.

In total, 1046 pairs of overtopping hazard observations and predictions were gathered across the 15 webcam sites, and some form of significant overtopping (hazard levels 1–3) was observed 35 times across 8 of the sites during the 2018-2019 winter. 1011 observations represented calm conditions where a low risk of overtopping was seen (hazard level 0), 18 observations were classed as hazard level 1 ('risk to pedestrians'), 12 were classed as hazard level 2 ('risk to pedestrians and property'), and 5 were classed as hazard level 3 ('risk to pedestrians, property, and vehicles'). Examples of webcam observations at Penzance promenade, Cornwall, UK, subjectively ranked from 0–3 are shown in Figure 7. In terms of a binary prediction of overtopping vs no-overtopping (where overtopping is ≥ hazard level 1), the forecast agreed with the observations 97% of the time (1013 out of 1046 observations). 2.5% of the predictions represented false alarms (false positives), while 0.7% represented a missed overtopping event (false negatives) where ≥ level 1 hazard was observed, but no warning at all was given by the forecast (Table 4-2). The false negatives represent 20% (7 of 35) of the overtopping that was observed, but were all events subjectively ranked as level 1, and none of the highest severity (level 2 and 3) events were missed by the system. Closer inspection of the false negatives indicates that the events often featured low levels of overtopping and were on the cusp of the lowest tolerable overtopping threshold.

In terms of the model's ability to accurately rank overtopping hazard, the predicted hazard level agreed exactly with the subjective classification for 37% (13 of 35) of the overtopping events, and was within 1 hazard level of the observations for 97% (34 of 35) of the overtopping events. Distributions of observed and predicted hazard level are presented in Figure 6, showing that the system predicted almost exactly the same number of low-severity events as were observed, but predicted more level 1 and 2 events than were observed. Interestingly, the forecast predicted only one level 3 event over the 2018-2019 winter, despite 5 such events being subjectively observed (these were all ranked at level 2 by the forecast). This may represent under-prediction of the highest hazard, or could indicate that some events were over-ranked by the observers, i.e. where a large amount of spray was observed, but less than level 3 overtopping volume occurred in reality (see Figure 7, panel D for a possible example of this).

Table 4-2. Number of agreements and disagreements between the observed and forecasted hazard level.

		Predicted (OWWL)	
		No overtop	Overtop
Observed (webcam)	No overtop	985 (94.2%)	26 (2.5%)
	Overtop	7 (0.7%)	28 (2.7%)

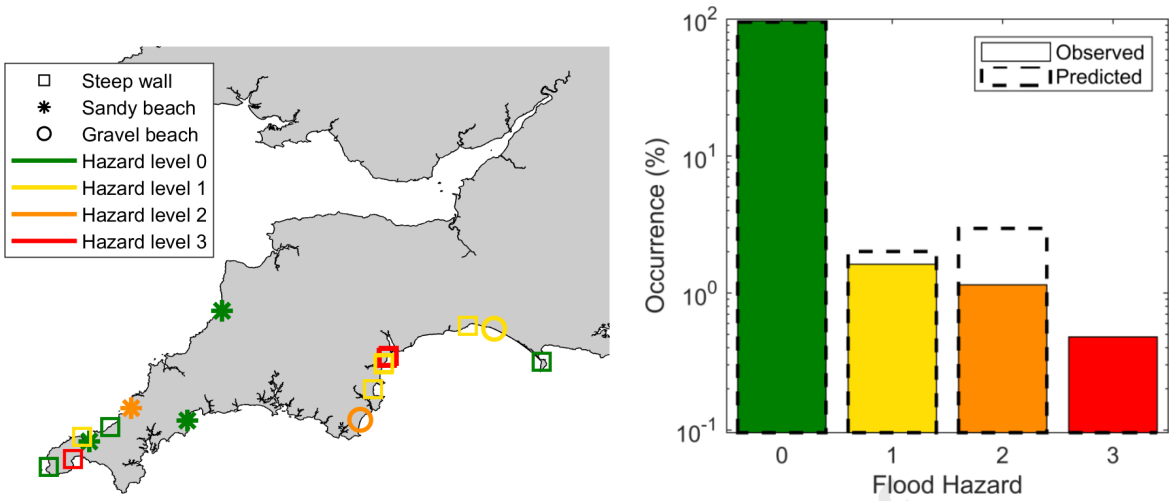

Figure 6. Left panel: locations used for validation of overtopping forecasts; anti-clockwise from top: Bude, Perranporth, Portreath, Hayle, St Ives, Sennen, Penzance, Pentewan Sands, Slapton Sands, Paignton, Teignmouth, Dawlish, Lyme Regis, West Bay, Chesil. Each location was viewed daily via webcam (Section 4.2), except for Perranporth and Slapton Sands, where site visits were undertaken during a single storm event at each site (Section 4.3). Symbols indicate the sea-defence type, while colour indicates the maximum observed hazard level during the monitoring period. Right panel: comparison of observed and predicted hazard ranking distributions.

Figure 7. Examples of subjectively ranked hazard level 0 (panel A – 21/03/19), level 1 (panel B – 28/11/18), level 2 (panel C – 28/11/18), and level 3 (panel D - 29/11/18) rated overtopping events at Penzance promenade, Cornwall, UK.

4.3 Wave overtopping validation – extreme storm events

The daily webcam observations described in Section 4.2 captured a number of overtopping events at seawalls, but only 1 overtopping event at a naturally defended site. Given that the method for forecasting overtopping at naturally defended sites (Section 3.6.2) has not been tested in its present configuration in the literature, additional validation was needed. Prior to the daily validation exercise, two significant storm events occurred which resulted in overtopping at a number of sites, including a gravel barrier at Slapton Sands, Devon, UK [48], and a sandy beach at Perranporth, Cornwall, UK. The locations of the two sites are shown in Figure 6. These two events provide useful additional case studies with which to verify the ability of SWEEP-OWWL to forecast overtopping at naturally defended sites.

Storm Eleanor occurred on the 3rd of January 2018, bringing Atlantic storm waves from the west. At Perranporth, a sandy beach in north Cornwall ($\tan\beta \approx 0.014$), waves peaked at H_{m0} = 7.8 m with T_p = 14 seconds (approximately 1:3.5 year return period) just after 06:00, coinciding with a high spring tide. Wave runup was predicted to exceed 2 m, which was enough to surpass the crest of the beach and overcome the access ramp and short wall (not considered a sea-defence structure) surrounding the adjacent car park. Photographs taken immediately after the event show flooded properties and sediment deposits in the car park (Figure 8), confirming that overtopping occurred. SWEEP-OWWL correctly forecasted that overtopping would occur, and the predicted level 2 hazard ('risk to pedestrians and property') compares well with the available overtopping evidence, despite the fact that the observations are from a sheltered area adjacent to the measured profile. During this event, overtopping was forecasted along most of the north coast but not on the south coast, and similar validation was obtained at Polzeath beach (location shown on Figure 8).

Storm Emma occurred on the 1st and 2nd of March 2018 and originated in the English Channel. The waves within Start Bay in South Devon reached H_{m0} = 5.8 m with a peak period of T_p = 10 s (Figure 9), which, given the rarity of large easterly waves represents a return period of around 1:50 years. The storm waves generated over 5 m of wave runup at the gravel barrier at Slapton Sands ($\tan\beta \approx 0.13$), which exceeded the crest of the barrier and caused significant wave overtopping and erosion. The overtopping deposited a significant amount of gravel on the A379 road (Figure 9), which traverses the crest of the barrier, confirming that overtopping occurred. SWEEP-OWWL forecasted a level 2 overtopping hazard, which could be deemed modest considering approximately 100 m of road was undercut and collapsed onto the beach. However, the collapse was largely due to erosion of sediment rather than overtopping, so level 2 hazard is deemed appropriate given the available evidence. During this event, overtopping was widely predicted along the south coast but not on the north coast, and additional verification of overtopping is available at several south-coast locations from newspaper reports.

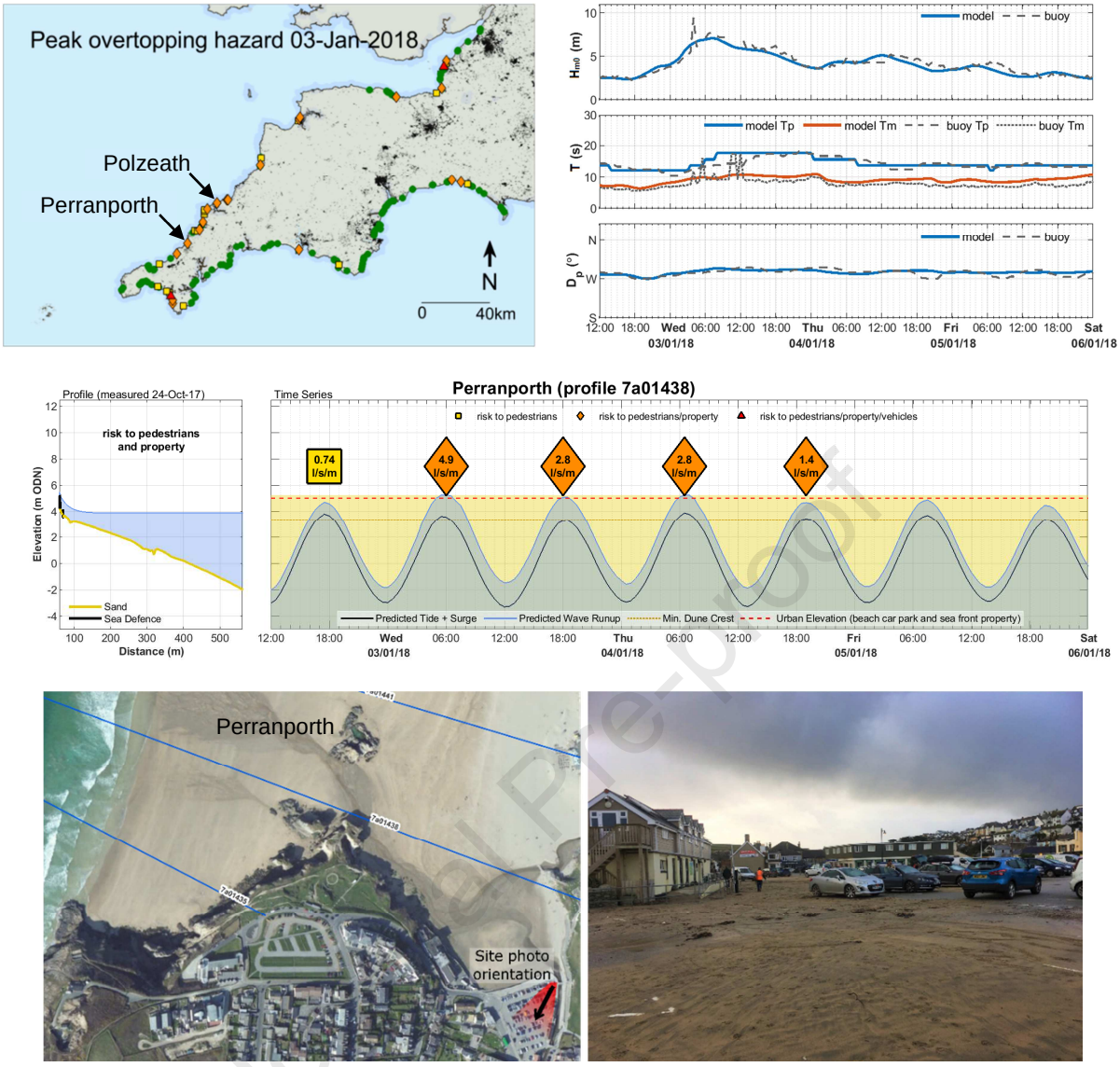

Figure 8. Forecasted wave conditions and overtopping for Storm Eleanor, 3rd Jan 2018. Top left: 3-day regional hazard forecast (see Figure 7 for legend). Top right: Forecasted and measured significant wave height (H_{m0}), peak (T_p) and mean (T_m) wave period, and peak wave direction (D_p) at -17 mODN depth contour at Perranporth beach. Middle left: Measured beach profile and predicted maximum still water and runup levels. Middle right: Time series of predicted water level and runup with overtopping volumes and hazard warnings. Dashed red line indicates the elevation of the beach car park. Bottom left: Location map showing Perranporth profile 7a01438 and beach car park. Bottom right: Overtopping was evident in the car park by sediment on the tarmac and through media reports of flooded properties to the right of the image.

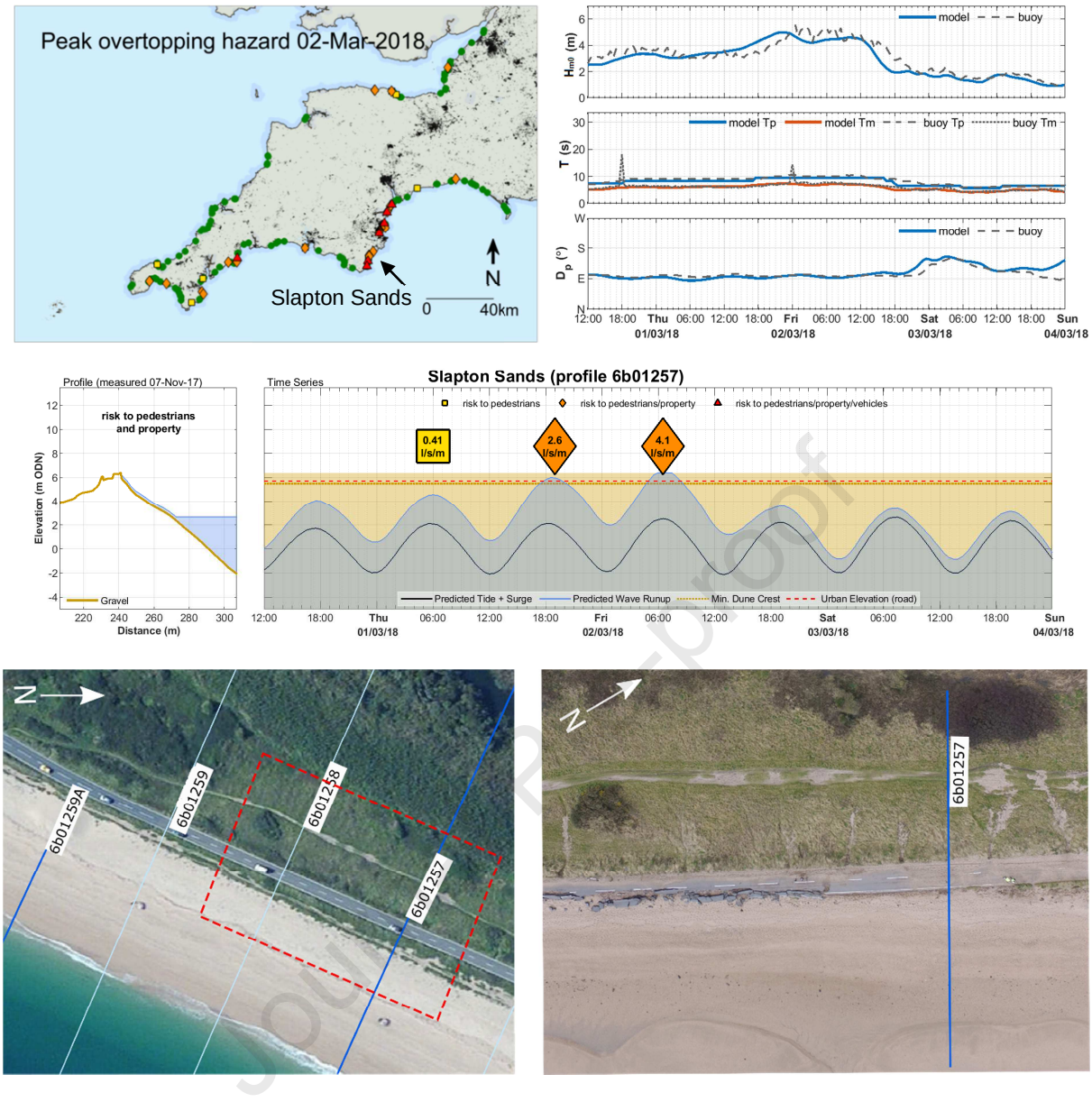

Figure 9. Forecasted wave conditions and overtopping for Storm Emma, 1st – 2nd March 2018. Top left: 3-day regional hazard forecast (see Figure 7 for legend). Top right: forecasted and measured significant wave height (H_{m0}), peak (T_p) and mean (T_m) wave period, and peak wave direction (D_p) at -12 mODN depth contour at Slapton Sands. Middle left: measured beach profile and predicted water level/runup. Middle right: time series of predicted water level and runup with overtopping volumes and hazard warnings. Dashed red line indicates the elevation of the road. Bottom: location of profile 6b01257 and the barrier before (bottom left) and after (bottom right) storm Emma; overtopping was evident from gravel deposited on the road and back barrier.

4.4 Sensitivity of overtopping to coastal profile shape

To test the sensitivity of predicted overtopping rate to variations in the measured coastal profile, Storm Emma (Section 4.3) was run over 24 coastal profiles measured at a single location at Teignmouth, Devon, UK, between May 2007 to November 2019. The site features a sandy beach ($0.013 < \beta < 0.039$) backed by a seawall (Figure 10) and is adjacent to a range of amenities and infrastructure, including a train line. The area is susceptible to shoreline rotation as well as cut-back during storms as a result of a bi-directional wave climate [49]. The beach elevation at the toe of the seawall at Teignmouth varied vertically by approximately 3 m over the 2007–2019 period (Figure 10, left panel), with intertidal profile volume (Figure 10, right panel) between the seawall and -2 mODN (approximately MLWS) varying between 68–263 m^3m^{-1}.

Under fixed boundary conditions from the peak of Storm Emma at this single coastal location, the predicted overtopping volume varies by an order of magnitude depending on which beach profile observation is selected (Figure 10, right panel). The predicted overtopping hazard ranges from low (hazard level 0) when the storm was run over a healthy beach profile, to the highest level of hazard (hazard level 3) when the same storm was run with a denuded beach. The variation in predicted overtopping is primarily due to the difference in wave breaker dissipation across the different intertidal profiles (Section 3.4), and resulting variation in wave setup and wave height at the toe of the seawall. This test indicates that wave overtopping is highly sensitive to the intertidal profile, proving the importance of a forecasting system that allows the coastal profile to be updated regularly, as per the present system.

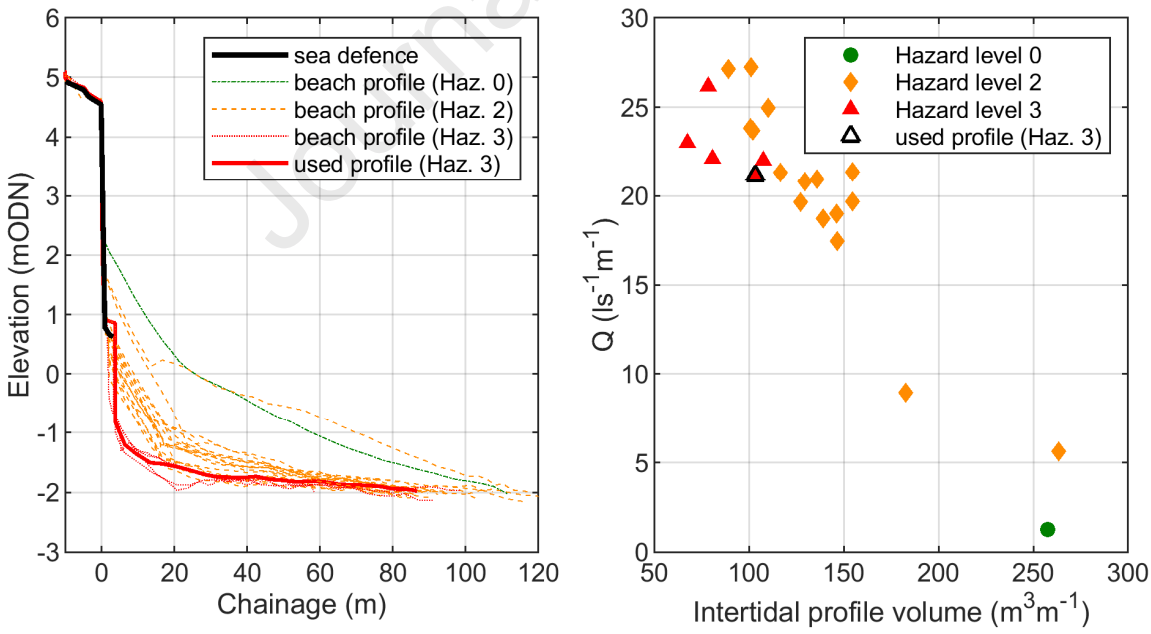

Figure 10. Left panel: 24 coastal profile measurements from a single location at Teignmouth beach. Line style is varied by the predicted wave overtopping hazard at the peak of Storm Emma. Right panel: predicted overtopping rate at the peak of Storm Emma for different profile observations at the same location, with symbol and colour varied by the predicted hazard level (Section 3.7). The most up-to-date profile measurement at the time of Storm Emma ('used profile') is shown with a solid line in the left panel and a bold symbol in the right panel.

4.5 Application to operational coastal management

For operational decision making – i.e. real-time forewarning of coastal overtopping – the SWEEP-OWWL forecast is automatically formatted into a series of PDF documents and emailed to a list of recipients each day (www.channelcoast.org/ccoresources/sweep/). Those recipients currently consist of Environment Agency flood response officers, and local authorities. The forecast is also broadcast more publicly via automated social media posts using the Twitter data API (www.twitter.com/@Coastal_Hazards). To generate these outputs, the forecast is first used to create a series of plots that present the predicted coastal flooding hazard at various spatial resolutions, from regional (that present maximum hazard over the 3-day forecast period for the whole of southwest England), to sub-regional (that present maximum hazard for 24 different sub-regions), and finally to individual coastal profiles (that present a time series of wave runup and overtopping hazard over the forecast period). Examples of regional-scale warnings and individual profile time-series plots are provided in Figure 8 and Figure 9.

4.6 Application to strategic coastal management

SWEEP-OWWL was primarily designed as an operational forecasting system, but can also be used for strategic purposes, for example, to identify areas that are currently vulnerable to coastal overtopping, or to evaluate the consequences of sea-level rise or increased storminess on coastal overtopping. Figure 11 shows regional hazard forecasts for Storm Emma and Storm Eleanor (Section 4.3), and compares them to a climate scenario where sea level is 1 m higher than present. This represents an extreme potential future sea-level rise, in line with the upper bound for the year 2100 from RCP8.5 of the UK Climate Projections (UKCP18, https://ukclimateprojections-ui.metoffice.gov.uk). For this simple example, the crest heights of natural and man-made defences have been kept at their present elevation; therefore, the freeboard of all coastal defences is assumed to decrease in line with sea-level rise.

According to this example, a westerly storm like Storm Eleanor (1:3.5 year return period) would result in many more locations in southwest England experiencing severe overtopping with sea level 1 m higher, including a number of locations on the sheltered south-facing coast that were predicted to be low hazard with sea level at its current position (Figure 11, upper panels). Similarly, an easterly storm like Storm Emma (1:50 year return period) would result in widespread and severe overtopping along most of the south coast with sea level 1 m higher (Figure 11, middle panels). Under the present climate, ~30 of the 184 studied profiles are predicted to have experienced overtopping > 1 $ls^{-1}m^{-1}$ during the two storms, with 5-10 profiles experiencing > 10 $ls^{-1}m^{-1}$ and the worst affected sites experiencing discharges of 100–200 $ls^{-1}m^{-1}$. With sea level 1 m higher, the model predicts that the storms would cause overtopping at more than 60-70 of the profiles, with 30–35 profiles experiencing discharges > 10 $ls^{-1}m^{-1}$, and peak overtopping rates could increase to more than 1000 $ls^{-1}m^{-1}$ (wier-flow conditions). With an additional 10% increase in H_{m0} (a hypothetical climate scenario, not predicted by UKCP18), overtopping rates for the two storms are predicted to increase only slightly (Figure 11, lower panel). Such scenario modelling can be used to quickly identify future overtopping ‘hot spots’, and could be repeated many times with varying combinations of forcing conditions and climate scenarios to provide statistical measures of coastal overtopping vulnerability. This is a simplistic approach to climate change modelling, as it does not properly account for the evolution of the coastline or for future updating of coastal defences. However,

such factors could be tested and would provide valuable information for the strategic management of coastal defences on a regional scale.

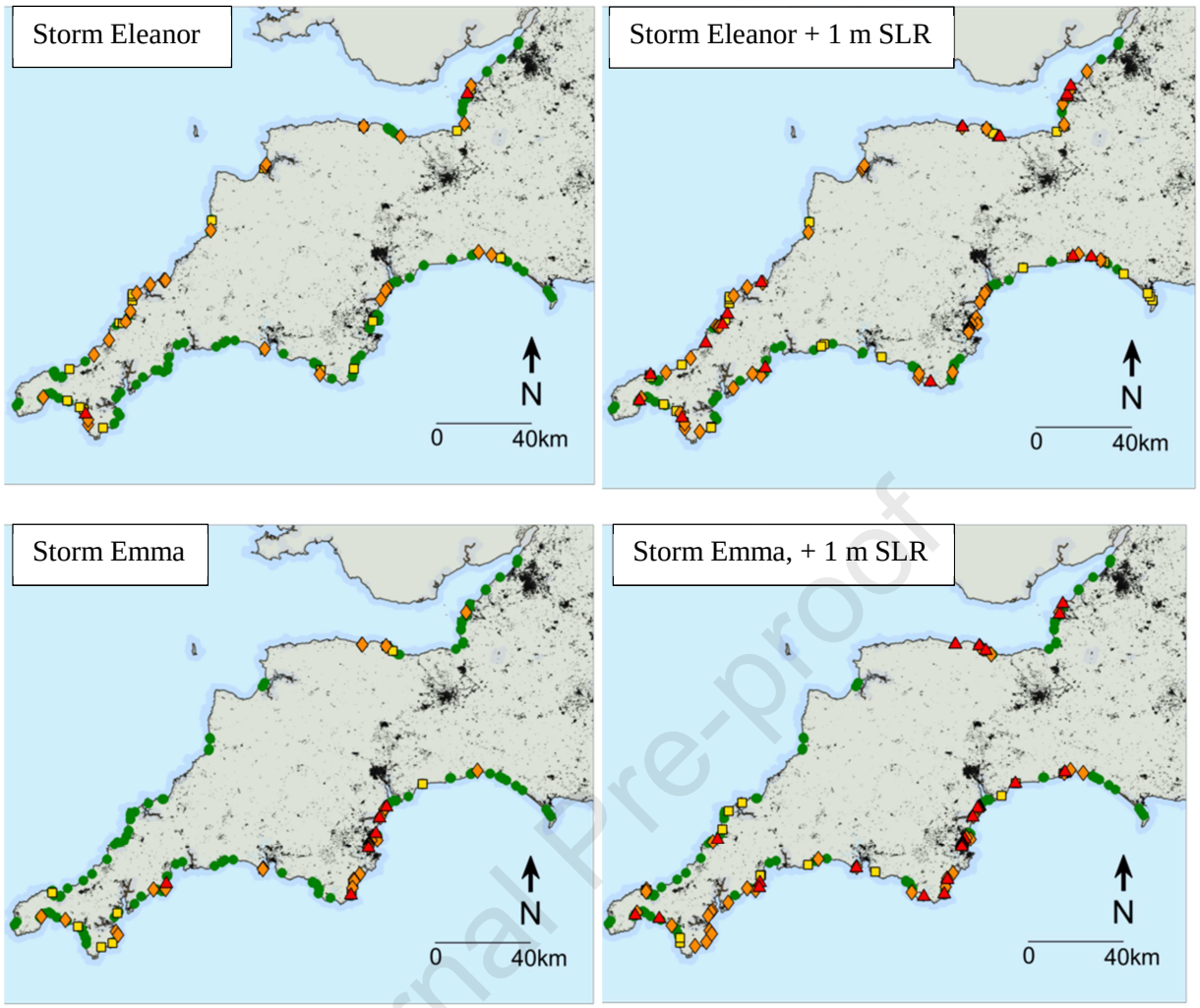

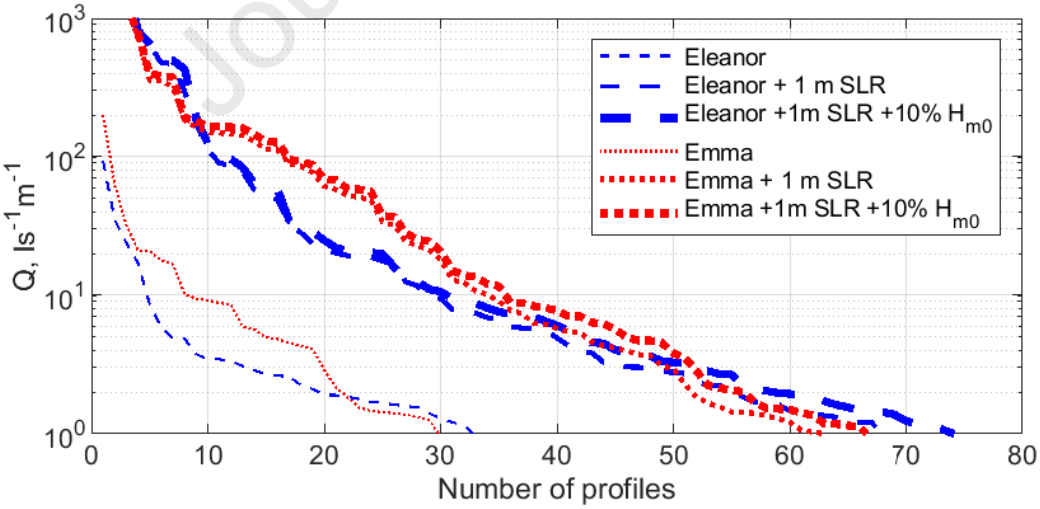

Figure 11. Strategic application of the SWEEP-OWWL overtopping forecast to explore the effects of Storm Eleanor (top panels) and Storm Emma (middle panels) with a future potential rise in sea level of 1 m. The lower panel shows the highest to lowest predicted levels of overtopping discharge around the southwest coast for the two storms, and shows the increase in predicted discharge with sea level 1 m higher and with an additional 10% increase in *Hmo*. More information on the two storms is provided in Section 4.3.

5 Discussion

In Section 4.4 it was demonstrated that overtopping rate is highly sensitive to the coastal profile that is used, and that using 'out-of-date' coastal profiles is likely to result in unacceptable levels of uncertainty in locations where the profile varies vertically by a metre or more. Existing methods to forecast coastal overtopping [1, 7] have relied on running a large number of off-line XBeach simulations with a single realisation of the coastal bathymetry. Although a more complete physical representation of the coastal hydrodynamics is possible using XBeach compared to the linear shoaling and empirical breaker, runup, and overtopping approach used in SWEEP-OWWL, the coastal bathymetry used in the XBeach based forecast systems would need to be updated regularly to provide relevant information, which would incur significant additional computation time with each update. In contrast, the on-line calculation of nearshore hydrodynamics and overtopping over the four-day prediction window (1-day hindcast plus 3-day forecast) in SWEEP-OWWL for all 184 profiles takes 16 minutes of computation time on a single computational core, and the profile database can be updated with no additional computational cost. This creates an opportunity to assimilate profile data whenever it becomes available, either through the present approach of utilising coastal monitoring data, or in future through the use of autonomous sensors.

This raises the question of whether overtopping is more sensitive to a complete representation of hydrodynamics (justifying the XBeach approach), or to the variability in the coastal profile (justifying the present approach), but such an assessment was beyond the scope of the present study. Either approach relies on the availability of accurate coastal boundary conditions – in SWEEP-OWWL, offshore boundary conditions are downscaled using a 1-km resolution hydrodynamic model in order to resolve differences in wave conditions within individual embayments. Across the European northwest shelf, forecasted waves and water levels are now freely available at a resolution of 1.5 km (https://marine.copernicus.eu/), which in most cases is sufficient to resolve hydrodynamics within individual embayments. It is therefore becoming increasing possible to run computationally efficient overtopping warning systems such as SWEEP-OWWL using freely available forcing conditions from a single desktop PC. However, there will always be a reliance on accurate and up-to-date coastal profile or bathymetric data, which are less widely available globally.

There are a number of ways that errors can be introduced to the forecasted wave runup or overtopping values in SWEEP-OWWL:

1. The boundary forcing data could be inaccurate
2. The Delft-3D model could introduce error in the water level, currents, and wave conditions
3. Wave propagation between the nearshore Delft-3D output nodes (10–20 m depth) and the coast ignores wave divergence, convergence, and dissipation over subtidal sandbars
4. The runup and overtopping equations each have their own uncertainty
5. The beach profile and sea-defence geometries are in some cases simpler than in reality
6. The beach profiles (updated twice a year) may have evolved between the measurement time and the time of a storm arriving, and may further evolve during the storm itself.

This study has attempted to quantify the degree of error introduced by (1) and (2), through validation of the 1-day ahead model predictions against wave and hydrodynamic data (Section 4.1). An attempt has also been made to characterise the expected level of accuracy in the 1-day ahead overtopping hazard predictions (Sections 4.2 and 4.3), which are subject to all the above listed sources of error. However, due to the difficulty of disentangling the contribution of error from sources (3) to (6) above, it is acknowledged that each individual aspect of the methodology has not been assessed for its error contribution. As such, it is not yet possible to provide robust confidence bounds on each forecasted runup and overtopping prediction. Despite this shortcoming, the level of accuracy of the hazard predictions is considered highly favourable for coastal management purposes, with 80% of the observed overtopping being predicted by the model, and the missed 20% of events representing low severity overtopping. Additionally, false alarms were only raised 2.5% of the time. Particularly encouraging is the fact that the classification of overtopping hazard (levels 0–3) either agreed with, or was within 1 classification level, of the overtopping observations nearly all of the time (97%). This indicates that the system is not only able to provide forewarning of coastal overtopping with approximately an 80% hit rate (and 100% hit rate for severe events), but also shows skill in differentiating between low severity and high severity overtopping events.

Another limitation of the system is that while it predicts overtopping rates and hazard, it does not yet attempt to predict coastal flooding extents. To predict flooding, forecasted overtopping rates would need to be fed into a flood propagation model, which would incur a significantly higher computational cost, and was not deemed feasible over the regional scale required from the present system. However, this may be a future option for specific high risk locations and could provide coastal managers with better quantification of the elements and extents at risk from coastal flooding during each storm.

Through developing a forecast system to predict overtopping for a variety of coastal situations, it is particularly apparent that further research is required to improve prediction of overtopping over naturally defended coastal profiles (beaches, dunes, and gravel barriers) where runup is well described [4, 32, 50] but available overtopping formulae [37-39] are yet to be validated. Equally, no satisfactory methods exist with which to predict wave overtopping at sea-defence structures that are fully emergent above still water level, yet considerable wave overtopping could occur in such cases if wave runup is significant and freeboard is low. Further research is required in both these areas in order to have a complete suite of coastal overtopping equations.

6 Conclusions

Current process-based models (e.g., XBeach) are not yet fully developed for the prediction of wave overtopping at coastal structures and cannot represent common sea-defence features such as wave return lips. Such models are also too computationally expensive to run in real-time for the 1000-km coastline of southwest England. To address these challenges, SWEEP-OWWL uses a coupled wave and current model (Delft-3D) combined with a computationally efficient suite of empirical equations to calculate nearshore wave shoaling, breaking, runup and overtopping. The system can be updated with the latest coastal profile measurements with no additional computational cost. The 1-km wave and hydrodynamic model takes approximately 2.5 hours to complete a 4-day simulation (1-day hindcast plus 3-day forecast), using 8 cores and parallel computing. The computation of nearshore hydrodynamics and overtopping for 184 coastal profiles then takes 16 minutes using a single computational core.

The accuracy of the overtopping predictions is considered highly favourable for coastal management purposes, with 80% of the observed overtopping events being predicted by the model 1-day ahead, and the missed 20% of events representing low severity overtopping (assessed using daily observations at 19 sites around SW England during the 2018/19 winter). Additionally, false alarms were only raised 2.5% of the time. Particularly encouraging is the fact that the classification of overtopping hazard (levels 0–3) agreed exactly with subjective observations half of the time and were within 1 classification level for 35 out of the 36 overtopping observations. This indicates that the system is not only able to provide forewarning of coastal overtopping with approximately an 80% hit rate (100% hit rate for severe events), but also shows skill in differentiating between low severity and high severity overtopping.

Wave overtopping is highly sensitive to the shape and volume of the intertidal beach profile. Under fixed boundary conditions from the peak of Storm Emma at a single coastal location, predicted overtopping rate varied by an order of magnitude depending on which beach profile observation was selected, with hazard level varying from low to high. In contrast to existing overtopping warning systems that have used only a single realisation of the coastal bathymetry, this finding provides justification for frequent coastal monitoring and a forecasting system that allows coastal profiles to be updated regularly, as per the present system.

Further research is required to improve prediction of wave overtopping volumes over naturally defended coastal profiles (beaches, dunes, and gravel barriers), where runup is well described but overtopping predictions are yet to be validated. Equally, no satisfactory methods exist with which to predict wave overtopping at sea-defence structures that are fully emergent above still water level, yet considerable wave overtopping could occur in such cases if wave runup is significant and freeboard is low. Equally, a future challenge for the development of SWEEP-OWWL is assimilating coastal profile data in real-time; this is currently updated twice a year and following severe storms by the regional monitoring programme, but could be updated much more frequently (i.e. daily) through the use of data assimilation from autonomous sensors.

The combined application of SWEEP-OWWL to operational (real-time forewarning) and strategic (climate change impacts) coastal management is currently helping to inform coastal management decisions during storms

across southwest England, and it is hoped that the approach will be developed further and applied to coastal regions across the UK and abroad, as a tool to improve the resilience of vulnerable coastal communities.

7 Acknowledgements

We would like to thank Roger Quinn, Keith Nursey, and Susan Connelly from the Environment Agency for supporting this project and collaborating with us on developing the model. Thanks also go to the Met Office for providing boundary forcing conditions. The research was funded by NERC through their Environmental Science Impact Programme (*South West Partnership for Environment and Economic Prosperity* (SWEEP) NE/P011217/1) and a Strategic Highlight Topics grant (*Physical and biological dynamic coastal processes and their role in coastal recovery* (BLUE-coast) NE/N015525/1).

References

[1] Van Dongeren, A., P. Ciavola, G. Martinez, C. Viavattene, T. Bogaard, O. Ferreira, . . . R. McCall, *Introduction to RISC-KIT: Resilience-increasing strategies for coasts.* Coastal Engineering, 2018. **134**: p. 2-9.

[2] Moftakhari, H.R., A. AghaKouchak, B.F. Sanders, D.L. Feldman, W. Sweet, R.A. Matthew, and A. Luke, *Increased nuisance flooding along the coasts of the United States due to sea level rise: Past and future.* Geophysical Research Letters, 2015. **42**(22): p. 9846-9852.

[3] Vitousek, S., P.L. Barnard, C.H. Fletcher, N. Frazer, L. Erikson, and C.D. Storlazzi, *Doubling of coastal flooding frequency within decades due to sea-level rise.* Scientific reports, 2017. **7**(1): p. 1399.

[4] Poate, T., R. McCall, and G. Masselink, *A new parameterisation for runup on gravel beaches.* Coastal Engineering, 2016. **117**: p. 176-190.

[5] Vousdoukas, M.I., L. Mentaschi, E. Voukouvalas, M. Verlaan, S. Jevrejeva, L.P. Jackson, and L. Feyen, *Global probabilistic projections of extreme sea levels show intensification of coastal flood hazard.* Nature Communications, 2018. **9**(1): p. 2360.

[6] Sallenger Jr, A.H., *Storm impact scale for barrier islands.* Journal of Coastal Research, 2000. **16**(3): p. 890-895.

[7] Barnard, P.L., M. van Ormondt, L.H. Erikson, J. Eshleman, C. Hapke, P. Ruggiero, . . . A.C. Foxgrover, *Development of the Coastal Storm Modeling System (CoSMoS) for predicting the impact of storms on high-energy, active-margin coasts.* Natural hazards, 2014. **74**(2): p. 1095-1125.

[8] Huang, C.-J., Y.-C. Chang, S.-C. Tai, C.-Y. Lin, Y.-P. Lin, Y.-M. Fan, . . . L.-C. Wu, *Operational monitoring and forecasting of wave run-up on seawalls.* Coastal Engineering, 2020. **161**: p. 103750.

[9] Zou, Q.P., Y. Chen, I. Cluckie, R. Hewston, S. Pan, Z. Peng, and D. Reeve, *Ensemble prediction of coastal flood risk arising from overtopping by linking meteorological, ocean, coastal and surf zone models.* Quarterly journal of the royal meteorological society, 2013. **139**(671): p. 298-313.

[10] Viavattene, C., J.A. Jiménez, O. Ferreira, S. Priest, D. Owen, and R. McCall, *Selecting coastal hotspots to storm impacts at the regional scale: a Coastal Risk Assessment Framework.* Coastal Engineering, 2018. **134**: p. 33-47.

[11] Harley, M.D., A. Valentini, C. Armaroli, L. Perini, L. Calabrese, and P. Ciavola, *Can an early-warning system help minimize the impacts of coastal storms? A case study of the 2012 Halloween storm, northern Italy.* Natural Hazards and Earth System Sciences, 2016. **16**(1): p. 209-222.

[12] Poelhekke, L., W.S. Jäger, A. Van Dongeren, T.A. Plomaritis, R. McCall, and Ó. Ferreira, *Predicting coastal hazards for sandy coasts with a Bayesian Network.* Coastal Engineering, 2016. **118**: p. 21-34.

[13] Roelvink, D., A. Reniers, A. Van Dongeren, J. Van Thiel de Vries, J. Lescinski, and R. McCall, *XBeach model description and manual.* Delft University of Technology, User Manual, Delft, The Netherlands, 2010.

[14] McCall, R.T., J.S.M.V.T. De Vries, N.G. Plant, A.R. Van Dongeren, J.A. Roelvink, D.M. Thompson, and A. Reniers, *Two-dimensional time dependent hurricane overwash and erosion modeling at Santa Rosa Island.* Coastal Engineering, 2010. **57**: p. 668-683.

[15] Van Dongeren, A., A. Bolle, M.I. Vousdoukas, T. Plomaritis, P. Eftimova, J. Williams, . . . J. Van Thiel de Vries, *MICORE: dune erosion and overwash model validation with data from nine European field sites*, in *Proceedings of coastal dynamics*. 2009. p. 1-15.

[16] Bolle, A., P. Mercelis, D. Roelvink, P. Haerens, and K. Trouw, *Application and validation of XBeach for three different field sites.* Coastal Engineering Proceedings, 2011. **1**: p. 40.

[17] Splinter, K.D. and M.L. Palmsten, *Modeling dune response to an East Coast Low.* Marine Geology, 2012. **329**: p. 46-57.

[18] O'Neill, A., L. Erikson, P. Barnard, P. Limber, S. Vitousek, J. Warrick, . . . J. Lovering, *Projected 21st century coastal flooding in the Southern California Bight. Part 1: development of the third generation CoSMoS model.* Journal of Marine Science and Engineering, 2018. **6**(2): p. 59.

[19] EurOtop, *Manual on wave overtopping of sea defences and related structures. An overtopping manual largely based on European research, but for worldwide application. Van der Meer, J.W., Allsop, N.W.H., Bruce, T., De Rouck, J., Kortenhaus, A., Pullen, T., Schüttrumpf, H., Troch, P. and Zanuttigh, B., www.overtopping-manual.com.* 2018.

[20] Donnelly, C., N. Kraus, and M. Larson, *State of knowledge on measurement and modeling of coastal overwash.* Journal of Coastal Research, 2006. **22**(4): p. 965-991.

[21] Castelle, B., V. Marieu, S. Bujan, K.D. Splinter, A. Robinet, N. Sénéchal, and S. Ferreira, *Impact of the winter 2013–2014 series of severe Western Europe storms on a double-barred sandy coast: Beach and dune erosion and megacusp embayments.* Geomorphology, 2015. **238**: p. 135-148.

[22] Saulter, A., C. Bunney, and J.-G. Li, *Application of a refined grid global model for operational wave forecasting*. 2016, Met Office Forecasting Research Technical Report.

[23] Roelvink, J.A. and G. Van Banning, *Design and development of DELFT3D and application to coastal morphodynamics.* Oceanographic Literature Review, 1995. **11**(42): p. 925.

[24] King, E.V., D.C. Conley, G. Masselink, N. Leonardi, R.J. McCarroll, and T. Scott, *The Impact of Waves and Tides on Residual Sand Transport on a Sediment□poor, Energetic and Macrotidal Continental Shelf.* Journal of Geophysical Research: Oceans, 2019. **124**: p. 4974–5002.
[25] O'Dea, E., R. Furner, S. Wakelin, J. Siddorn, J. While, P. Sykes, . . . H. Hewitt, *The CO5 configuration of the 7 km Atlantic Margin Model: large-scale biases and sensitivity to forcing, physics options and vertical resolution.* Geoscientific Model Development, 2017. **10**(8): p. 2947-2969.
[26] Battjes, J.A. and M.J.F. Stive, *Calibration and verification of a dissipation model for random breaking waves.* Journal of Geophysical Research: Oceans, 1985. **90**(C5): p. 9159-9167.
[27] Janssen, T.T. and J.A. Battjes, *A note on wave energy dissipation over steep beaches.* Coastal Engineering, 2007. **54**(9): p. 711-716.
[28] Battjes, J.A. and J. Janssen, *Energy loss and set-up due to breaking of random waves*, in *Coastal Engineering 1978*. 1978. p. 569-587.
[29] Baldock, T.E., P. Holmes, S. Bunker, and P. Van Weert, *Cross-shore hydrodynamics within an unsaturated surf zone.* Coastal Engineering, 1998. **34**(3-4): p. 173-196.
[30] Longuet-Higgins, M.S. and R.W. Stewart, *Radiation stress and mass transport in gravity waves, with application to 'surf beats'.* Journal of Fluid Mechanics, 1962. **13**: p. 481-504.
[31] Van Rijn, L.C., *Unified view of sediment transport by currents and waves. I: Initiation of motion, bed roughness, and bed-load transport.* Journal of Hydraulic engineering, 2007. **133**(6): p. 649-667.
[32] Stockdon, H.F., R.A. Holman, P.A. Howd, and A.H. Sallenger, *Empirical parameterization of setup, swash, and runup.* Coastal Engineering, 2006. **53**: p. 573-588.
[33] Battjes, J.A. *Surf similarity*. in *14th International Conference on Coastal Engineering*. 1974. Copenhagen.
[34] McCall, R.T., G. Masselink, T.G. Poate, J.A. Roelvink, L.P. Almeida, M. Davidson, and P.E. Russell, *Modelling storm hydrodynamics on gravel beaches with XBeach-G.* Coastal Engineering, 2014. **91**: p. 231-250.
[35] Altomare, C., T. Suzuki, X. Chen, T. Verwaest, and A. Kortenhaus, *Wave overtopping of sea dikes with very shallow foreshores.* Coastal Engineering, 2016. **116**: p. 236-257.
[36] Bruce, T., J. Pearson, and W. Allsop. *Violent wave overtopping - extension of prediction method to broken waves*. in *Proc. Coastal Structures 2003*. 2003. ASCE, Reston, Virginia.
[37] Hancock, M.W. and N. Kobayashi, *Wave overtopping and sediment transport over dunes*, in *Coastal Engineering 1994*. 1995. p. 2028-2042.
[38] Kobayashi, N., Y. Tega, and M.W. Hancock, *Wave Reflection and Overwash of Dunes.* Journal of Waterway, Port, Coastal, and Ocean Engineering, 1996. **122**(3): p. 150-153.
[39] Tanaka, H., Suntoyo, and T. Nagasawa, *Sediment intrusion into Gamo Lagoon by wave overtopping*, in *Coastal Engineering 2002: Solving Coastal Conundrums*. 2003, World Scientific. p. 823-835.
[40] Figlus, J., N. Kobayashi, C. Gralher, and V. Iranzo, *Wave overtopping and overwash of dunes.* Journal of Waterway, Port, Coastal, and Ocean Engineering, 2010. **137**(1): p. 26-33.
[41] Roelvink, D., A. Reniers, A.P. Van Dongeren, J.v.T. de Vries, R. McCall, and J. Lescinski, *Modelling storm impacts on beaches, dunes and barrier islands.* Coastal Engineering, 2009. **56**: p. 1133-1152.
[42] De Waal, J.P. and J.W. Van der Meer. *Wave runup and overtopping on coastal structures.* in *3rd International Conference on Coastal Engineering*. 1992. Venice, Italy.
[43] Davidson, M.A., R.P. Lewis, and I.L. Turner, *Forecasting seasonal to multi-year shoreline change.* Coastal Engineering, 2010. **57**: p. 620-629.
[44] Sutherland, J., A.H. Peet, and R. Soulsby, *Evaluating the performance of morphological models.* Coastal Engineering, 2004. **51**: p. 917-939.
[45] Brown, J., M. Yelland, R. Pascal, T. Pullen, P. Bell, C. Cardwell, . . . G. Shannon, *WireWall: a new approach to coastal wave hazard monitoring.* 2018.
[46] Pullen, T., E. Silva, J. Brown, M. Yelland, R. Pascal, R. Pinnell, . . . D. Jones, *WireWall–laboratory and field measurements of wave overtopping.* 2019.
[47] Almeida, L.P., G. Masselink, R. McCall, and P. Russell, *Storm overwash of a gravel barrier: field measurements and XBeach-G modelling.* Coastal Engineering, 2017. **120**: p. 22-35.
[48] McCarroll, R.J., G. Masselink, M. Wiggins, T. Scott, O. Billson, and D. Conley, *Gravel beach cross-and alongshore response to an extreme event: beach length and headland proximity controls*, in *Proc. of Coastal Sediments 2019*. 2019, World Scientific.
[49] Wiggins, M., T. Scott, G. Masselink, P. Russell, and N.G. Valiente, *Regionally-Coherent Embayment Rotation: Behavioural Response to Bi-Directional Waves and Atmospheric Forcing.* Journal of Marine Science and Engineering, 2019. **7**(4): p. 116.
[50] Stockdon, H.F., D.M. Thompson, N.G. Plant, and J.W. Long, *Evaluation of wave runup predictions from numerical and parametric models.* Coastal Engineering, 2014. **92**: p. 1-11.

Highlights

- We develop and test an efficient forecast system for wave overtopping forewarning
- Predicts waves, water levels, and overtopping for 1000 km coastline on a desktop PC
- Correctly predicted the presence or absence of wave overtopping with 97% accuracy
- Can be updated with latest coastal profile data with no extra computational cost
- This is shown to improve the predicted overtopping rate by an order of magnitude

Declaration of interests

☒ The authors declare that they have no known competing financial interests or personal relationships that could have appeared to influence the work reported in this paper.

☐The authors declare the following financial interests/personal relationships which may be considered as potential competing interests: